

Photosynthetic traits in the C4 species *Cleome gynandra*.



Author: Beatrice Landoni, MPS student, WUR (NL)

Supervisors: Eric Schranz – Biosystematics, WUR (NL)
Jeremy Harbinson – Horticulture and Product physiology, WUR (NL)

Wageningen University, WUR
Academic Year 2016 – 2017

Table of Contents

1. Introduction	1
1.1. An overview of photosynthesis	1
1.2. C4 photosynthesis	3
1.3. Cleome gynandra as a model species.....	3
1.4. C. gynandra: Phenotypic variation	4
1.5. Phenotyping photosynthesis	4
1.6. Photosynthetic traits	5
2. Research aim and questions.....	9
3. Material and Methods.....	10
3.1. Data acquisition.....	10
3.2. Plant material	10
3.3. Greenhouse experiment.....	10
3.4. Climate chamber experiments – D2 and B6	11
3.5. Data analysis.....	12
4. Results	15
4.1. Greenhouse experiment.....	15
4.2. D2 and B6 experiment.....	19
5. Discussion.....	21
5.1. Differences between African and Asian lines	21
5.2. rETR	21
5.3. Pigments and photosynthesis	23
5.4. Climate chamber experiments	24
5.5. Further developments.....	25
6. Conclusions	25

Summary

Cleome gynandra is a species deserving attention for different reasons; it could be useful to sustain local economy and enhance food security where not much else can be grown [1]. But *C. gynandra* is also relevant for another reason: it is the closest C4 species to the Brassicaceae family, therefore to the model species *Arabidopsis* [2–6]. The information coming from *Arabidopsis* may be useful for understanding how C4 photosynthesis works in closely related C4 species such as *Cleome gynandra*. Before achieving this, *Cleome gynandra* needs to be phenotyped for different traits and its genome needs to be studied [2]. The aim of this thesis is to phenotype photosynthetic traits for a diversity panel of 71 different accessions of *Cleome gynandra*. An earlier study grouped these lines into 3 clusters based on carotenoid and tocopherol content, with one cluster mainly composed by Asian accessions and the other one by African accessions. We have screened photosynthetic traits such as the relative electron transport rate (rETR) between PSII and PSI and the chlorophyll reflectance of leaves (SPAD) to assess the species' potential in terms of photosynthesis, and in particular to see if differences in rETR occur between African and Asian accessions. We found that Asian accessions have a higher rETR under the growth conditions used for this study. This finding is encouraging as it could mean that genetic variation is present for photosynthetic traits such as rETR. Understanding the mechanisms involved in photosynthesis and knowing the genes regulating this process is extremely important. C4 plants in particular are, at least under high temperatures and low CO₂ availability, more efficient in terms of light use and CO₂ conversion to biomass [7,8]. This makes the C4 pathway interesting for crops grown in sub-tropical and tropical climates as crop yields could be increased thanks to a more efficient photosynthetic pathway, especially in view of climate change [8,9]. But there is still much to be learned about the genetic bases of photosynthesis. Studying photosynthetic phenotypes is in fact complex; there are many genes that can vary with light, but also water and carbon dioxide availability. New techniques such as chlorophyll fluorescence imaging are now available to screen thousands of accessions in a very short time [10]. In this study we tried to use two recently developed instruments, MultispeQ [11], a field tool, and Phenovator [12], an automated system, to describe rETR and leaf chlorophyll content in *Cleome* using chlorophyll fluorescence as a proxy. A further step of this study would be to compare *Cleome*, a C4 species, with *Arabidopsis*, a C3 species.

1. Introduction

1.1. An overview of photosynthesis

Photosynthesis is described as the process by which plants convert energy and inorganic matter into biomass, or the process which uses light to fix atmospheric carbon. When studying photosynthesis in plants, light is qualitatively described as PAR (Photosynthetic active radiation), a particular fraction of the solar radiation ranging from 400 to 740nm [13]. Light can also be quantified as PPFD (Photosynthetic Photon Flux Density), which has units of moles (of photons) per square meter per second – in practice, micromoles are used in place of moles. Variation in light quantity and quality can be due to large scale factors such as geographic position, weather conditions and climate, and the time of day, but it can be also due to canopy structure because of shading and leaf absorbance; for example near infra-red light (longer wavelength) can penetrate more deeply into the canopy or into the leaf layers than blue or red wavelengths [14]. Being unable to cope with all sorts of light intensities and qualities with the same efficiency, plants have long-term and short-term adaptation mechanisms in response to light variations. These processes mainly aim to capture more energy or to dissipate the excess energy they receive without resulting in damage to the photosynthetic apparatus [15]. Sometimes energy dissipation by metabolic and non-metabolic processes is not enough and excess light can actually damage the photosynthetic apparatus and other organelles in the chloroplast. Nonetheless, there are various grades of adaptation to different light qualities and intensities or other environmental conditions; variation was found at between-species level (e.g. the different photosynthetic types as C3, C4, CAM), but also within a species [16,17] or within the same individual due to shading in the plant canopy [14]. For example it was shown that the photosystems' dimension and ratio (PSII/PSI) or the ratio between different pigments can change in order to use light in the most efficient way [14].

In the leaf, light is mainly collected by photosynthetic pigments such as chlorophylls a and b or by carotenoids. These pigments are bound to a range of proteins which are specifically aggregated into two types of super-complex – photosystems I and II (PSI and PSII), which are, in turn, situated in the chloroplast membranes of a leaf. PSI and PSII are formed by the respective reaction centers and by the LHCs (light harvesting complexes), where light is harvested. After being harvested, the energy is transferred from chlorophyll to chlorophyll via electron excitation to the reaction centers formed by pairs of particular chlorophylls (P680 for PSII and P700 for PSI) [15]. PSII is responsible for the split of H₂O into O₂, protons and electrons. The accumulation of protons in the thylakoid lumen and the electron flow from PSII to PSI are used for the synthesis of ATP by the ATP-synthase and the reduction of NADP [18].

1.1.1. Photosynthetic pigments

Chlorophylls are among the pigments mainly involved in light harvesting and energy transfer; even though this relation is not elementary. First of all, there are different kinds of chlorophylls, the most important being chlorophyll a (Chla) and chlorophyll b (Chlb); while both Chla and b are present in light harvesting complexes, Chla is also present in reaction centers. The ratio between Chla and Chlb can vary depending on the adaptation of the plant to different light intensities. With high light intensities, plants tend to have a higher Chla/Chlb ratio, since the LHC size tends to be reduced in order to harvest less light. Another reason for which the Chla/Chlb ratio can change is that the PSII/PSI ratio changes depending on the quality of light received by the leaves [14,19].

Different types of carotenes (e.g. beta carotenoids) and xanthophylls are also involved in light harvesting, contributing to enrich the spectrum of light that plants can use. Moreover, the xanthophyll cycle involving violaxanthin and zeaxanthin, is fundamental for photoprotection since it enhances non-photochemical quenching (NPQ) [15,20].

1.1.2. Photosynthetic reactions

1.1.2.1. Light reactions

When light hits chlorophyll molecules, an electron is lifted to a higher energy level forming an excited state. This excited state can migrate from one chlorophyll molecule to another to eventually reach P680 or P700 in the reaction-centers of either photosystems II and I. When this happens in PSII, the excited special chlorophyll can be oxidized thanks to redox reactions involving the split of H₂O – the first step of photosynthetic electron transport [18]. During this process, energy loss can happen: the pigments responsible of light harvesting cannot cope with all the solar energy they receive due to the wavelength range in which they operate. The main reason is that there is an energy gap between the relaxed and the excited state of an electron. When the energy provided to an electron by a photon is smaller or equal to the energy gap, the electron cannot pass to the excited state; at the same time, when excessive for the transition, the energy in surplus will be quickly dissipated before it can be used for photosynthetic reactions. In plants' chlorophylls, the energy gap is already fulfilled by photons in the red-spectrum of light (~700 nm). Even if shorter wavelengths can ideally provide photons with more energy than longer wavelengths, the free-energy actually available for the photosynthetic system will be the one remaining after the excess has been dissipated as fluorescence or heat [13].

The charge separation events mentioned above are connected to a more extensive electron transport chain that results in the oxidation of water, the reduction of NADP, and the translocation of protons across the thylakoid membrane to form a proton gradient (ΔpH) necessary to produce ATP. The electron transfer starting from the reaction center of PSII is slower than the energy transfer from the LHCs to the reaction center. Under high light intensities (or other sources of stress), the reaction centers may saturate and stop using the energy collected by the LHCs. This energy then accumulates in the photosynthetic membrane and possibly causes photodamage to which PSII is particularly sensible. The chlorophylls in the reaction centers can start to oxidize the nearby proteins or forming triplets causing the bleaching of the same reaction center. Conformational changes in the LHCs and NPQ are preventive mechanisms, that may be related to each other. NPQ is a complex process in which different players are involved, for example the transmembrane ΔpH and the xanthophyll cycle, underlying the importance of other pigments than chlorophylls in photosynthesis [15].

1.1.2.2. Dark reactions

The NADPH and ATP produced during the light reactions are later used in dark reactions such as the Calvin-Benson cycle where CO₂ is fixed via enzymatic processes [18]. Different photosynthetic types (e.g. C₃, C₄, CAM) have different needs in terms of ATP and NADPH to complete one cycle and fix one molecule of CO₂ [13]. The Calvin-Benson cycle starts with the fixation of CO₂. The catalyzer of this process, RuBisCo, uses CO₂ to transform the Ribulose-1,5-biphosphate (RuBP) into 3-phosphoglycerate. The phosphoglycerate is then reduced by other enzymes that use ATP and NADPH to finally produce glyceraldeide-3-phosphate (G3P); part of this is transferred to the cytosol where glucose and other organic compounds are synthesized. ATP is also needed in the final step of the cycle where Ribulose-1,5-biphosphate is again synthesized from the rest of the G3P coming from the previous step [21].

Despite its fundamental function, RuBisCo is not CO₂ specific since it can also bind to O₂. When this happens, RuBisCo oxidize RuBP with O₂ producing phosphoglycolates that, contrary to phosphoglycerates, cannot be used in the Calvin-Benson cycle; instead, they enter a C₂ cycle, a less efficient way of fixing CO₂ that gives toxic compounds such as ammonia as side product. This process is called photorespiration and it can arise whenever the concentration of oxygen in the plant cell is higher than CO₂ concentration. RuBisCo evolved around 2800 million years ago, with the rise of the ancestral C₃ pathway, when atmospheric CO₂ was more abundant than today compared to O₂; this may explain a lack of selective pressure towards a higher RuBisCo specificity for CO₂ [22]. The different photosynthetic types (e.g. C₃, C₄ and CAM) are mainly defined according to the way the plant copes with this problem.

1.2. C4 photosynthesis

Under conditions where photorespiration is theoretically favored, C4-species are more efficient at fixing CO₂ than C3-species since the C4 pathway works to increase the concentration of CO₂ around RuBisCo, actually avoiding photorespiration. Environmental conditions favoring photorespiration can be low atmospheric CO₂ levels, but also high temperature, drought and salinity that can trigger stomatal closure and reduce transpiration with the consequence that O₂ accumulates inside the leaf. Low atmospheric CO₂ levels in particular played an important role in the rise of the C4 pathway probably around 30 million years ago, but other factors such as temperature, water availability and soil properties determined the global distribution of C4 species nowadays [8,13,22]. For example, *Cleome gynandra* grows in sub-tropical environments where high temperatures and dry periods can occur [1,23].

As already said, when RuBisCo binds O₂ instead of CO₂, phosphoglycolates are produced and have to be processed via the photorespiratory, or photosynthetic carbon oxidation pathways. Contrary to C3 species, the majority of plants doing C4-photosynthesis can sensibly reduce photorespiratory processes having two specialized cell types in the leaves: the bundle sheath cells (BS) where CO₂ is actually fixed by Rubisco and the mesophyll cells (M), where CO₂ is firstly fixed by PEPC (Phosphoenolpyruvate carboxylase) and then diffused to the bundle sheath cells [4,8]. This is how Rubisco avoids oxygen-binding. Nonetheless, the compartmentalization of RuBisCo has a cost; while C3 species needs roughly 3 ATP and 2 NADPH molecules to complete one Calvin cycle and fix one molecule of CO₂, C4 plant needs about two more ATPs/cycle to keep the CO₂ concentration higher in the BS cells [13].

If this is a general distinction between the C3 and C4 photosynthetic types, there are also differences within the C4 group. Different C4 types are defined depending on the morphology of BS and M cells and on the enzyme that decarboxylates the organic acid after diffusion in the BS cells, previously produced by PEPC. For instance *Cleome gynandra* was shown to be a NAD-dependent malic enzyme (NAD-ME) species, but the activity of the other enzymes (NADP-ME and PCK) was detected as well [4].

1.3. *Cleome gynandra* as a model species

1.3.1. Description

Cleome gynandra is an annual C4 herb, branched, with a long tap root, compound leaves and a member of the plant family Cleomaceae. This species produces racemes bearing flowers with stamens characterized by long filaments, reason for which it is commonly called “cat’s whiskers” or “spiderplant”, and it reproduces either via self- or cross-pollination [24]. The species grows in hot tropical areas; it has a wide geographical range from Africa (its origin place) to the Americas and Southern Asia. Often considered a weed, *C. gynandra* is sometimes grown for food in Africa and for oil extraction in Asia [24]. This species does not have particular requirements for soil and nutrients, but regarding its performance under drought, different behaviors have been described [1]. *Cleome gynandra* is believed to have beneficial properties, especially for pregnant women and it is thought to be rich in carotenoids [1,24].

1.3.2. A C4 model

Cleome gynandra is a potentially interesting C4 model: it is closely related to Arabidopsis and different photosynthetic types have been found in the Cleomaceae family: C3 and C4 species (e.g. *Tarenaya hassleriana* and *Cleome gynandra*), but also possible intermediates between these two (e.g. *Cleome foliosa*) [4]. Secondly, the genome of *C. gynandra* is quite small and its life-cycle shorter when compared to Corn or Flaveria. Up to now in fact, only *Zea mays* and *Flaveria graminis* have been commonly used as C4 models, despite the C4 pathway independently evolved in more than 60 different angiosperm lineages [6]. The use of Corn and Flaveria as C4 models has some more drawbacks. Many genetic resources are available for corn, but its genome is large, its cycle long and it is not closely related to the two species for which the genome has already been sequenced: *Arabidopsis thaliana* and *Oryza sativa*. Comparative studies are hardly feasible. Flaveria has the same problems, plus the fact that not many genetic resources are available for this species [2].

1.3.3. Genome and polyploidy in Brassicales

Using *C. gynandra* as a C4 model would allow comparisons with Arabidopsis, but for this purpose it is important to know how the genomes of these two species are related. The Cleomaceae is a sister family of Brassicaceae where the C3 species *A. thaliana* belongs. Both families are part of the order Brassicales, and they both underwent a whole genome duplication (At- β). The Brassicaceae family is again characterized by a whole genome duplication named At- α , while the Cleomaceae family probably underwent a genome triplication (Cs- α or Th- α) [5,6]. Th- α happened before the divergence of *Tarenaya hassleriana*, a C3 species, and *Cleome gynandra*, a C4 species. To understand how the C4-type evolved in the Cleomaceae family, it can be useful to compare Brassicaceae species such as Arabidopsis (C3), to Cleomaceae species, such as Tarenaya (C3) and Cleome (C4), being the two families so closely related. From this comparison [6], what emerges is an apparent increase in the retention of gene-duplicates related to photosynthetic processes for the Cleomaceae family in general; on the other hand, despite the fact that Tarenaya is a C3 and Cleome a C4 species, the two species don't seem to differ for retention in duplicates of genes related to photosynthesis. Even though, it was noticed that a more stringent transcriptional regulation of C4-cycle genes takes place in *C. gynandra*.

1.4. *C. gynandra*: Phenotypic variation

Cleome gynandra is not only interesting in the context of photosynthesis, as it is variable for different traits at phenotypic level, ranging from the morphological to the biochemical. To date, little effort was directed to seed preservation and creating core collections for this species [1,23]. The creation of core collections could be for example improved by further exploiting genomic and phenotypic data. In this respect, recent studies have focused on characterizing accessions, especially for agronomic and nutritional traits, such as productivity, days to flowering or mineral content. [23,25]. Interesting features that could relate to photosynthesis already analyzed in these studies are chlorophyll content, stem color and carotenoids content. For instance, variation was found for chlorophyll content [23], even among different accessions coming from a relatively small area. The high nutritional value of Cleome and its high variability make Cleome a species with the potential of becoming a crop.

1.5. Phenotyping photosynthesis

1.5.1. Variation in photosynthesis

Photosynthesis is a broad process determining both determining the physiology and the architecture of a plant and is strongly influenced by these characteristics and environmental conditions. Therefore, it can be hard to determine what a photosynthetic trait is and what is not, or to take observations for these traits, reducing the environmental disturbance to the minimum. It is true that we can distinguish different photosynthetic pathways (e.g. C3, C4 and CAM), but this is a very general classification. What happens when focusing on the individual plant or even on single leaves?

Up to now, limited research has focused on photosynthesis in relation to its phenotypic and genotypic variation, especially in terms of natural variation [16]. Photosynthetic proteins such as Rubisco were shown to be highly conserved across species and this led to the opinion that there was not much variation for photosynthetic traits in general [8,16]; in addition, the photosynthetic phenotype is an elusive trait and its observation requires sophisticated measurement techniques [10,16].

This also influenced the way breeders were looking at photosynthesis, only studying and breeding for traits indirectly related to photosynthesis, and especially related to plant architecture or morphological features. For example the leaf inclination or the leaf area index (LAI) had been target traits for breeders, but these traits affect more the quantity and quality of light that it is used by the plant, than the actual way the photosynthetic apparatus process this light during photosynthesis [9].

Nonetheless, natural variation is present in terms of photosynthetic efficiency at leaf level as shown in different studies [16,17,26,27]. It can change even within one single individual; for example shade and sun leaves or leaves of different ages can be different in terms of PSI and PSII ratio and the type of light they use [14,19,28]. But it is important to keep in mind that the photosynthetic rate of a single leaf may not represent

the plant yield. Much more complex interactions with other factors, such as plant architecture, determine a plant's production.

1.5.2. Different tools for chlorophyll fluorescence measurements

Measuring photosynthesis as carbon dioxide fixation is difficult, but parameters derived from chlorophyll fluorescence can be a proxy for it, allowing fast screening of several plants, in particular when using chlorophyll fluorescence imaging [10]. Chlorophyll fluorescence is a quantitative trait, therefore determined by many genetic factors and of course influenced by the environment. To give the observed variation a name, it is essential to screen several individuals and repeat the measurements several times per day and over multiple days. It is also important to measure plants in a changing environment, especially in terms of light, to simulate outside conditions where light quality and quantity are always shifting [10,11]. This is not often and easily done since there is a trade-off between minimizing the variation due to environmental effects and reproducing realistic growth conditions. For example, when studying photosynthetic efficiency in a field-crop, it may be useful to know how different genotypes actually perform in the field; on the other hand, with a constantly changing light and heterogeneous distribution of water and nutrients in the ground, together with the difficulty of measuring many plants spread on a big area, it may be hard to gather relevant data.

Despite this, when designing an experiment that considers what may be an undesired source of variation, there are instruments such as portable pulse modulated fluorometers that can measure chlorophyll fluorescence in the field with a relatively high throughput. The recently developed MultispeQ can measure PSII efficiency and chlorophyll content for example, while also detecting light intensity, temperature and relative humidity [11]. The drawbacks are that speed and accuracy of the measurements depend on the operators, only one part of a leaf is actually observed per measurement and less physiological parameters can be taken into account than with fluorescence imaging, another useful technique to gather this type of data. In a recent work, Flood et al. (2015) described the Phenovator. This system makes use of a 2D camera recording the plants' fluorescence. The camera moves along two perpendicular axes over the table in the climate chamber where the plants are growing. This method allows high-throughput imaging of hundreds of plants, several times per day, sensibly reducing variability due to the environment that may hide the effect of different genotypes. Even though, it is necessary to remember that a genotype performing well in such environment may not perform equally well in the field. Moreover, the Phenovator works for plants that can be reduced to a 2D-image, but it could be less appropriate for plants which require three dimensions to be accurately described [12,27].

Although fluorescence imaging and portable fluorometers seem to be promising, the most common method used for fluorescence measurements follows quite a different approach. The measurements are always taken with a pulse amplitude fluorometer, but in this case the leaves are detached from the plant, usually dark-adapted, and only a small part of their surfaces is actually measured. Even if the accuracy of the measurement is great, the information it bears may not be representative of the actual status of the measured plant. Moreover, this method being destructive, it is a source of stress for the plants and the same plants can only be measured a reduced amount of times during their cycles.

1.6. Photosynthetic traits

Chlorophyll fluorescence is one of the phenomena observed to indirectly measure the photosynthetic efficiency of a plant as many useful parameters related to photosynthetic efficiency, in particular PSII efficiency, can be derived via chlorophyll fluorescence. Other traits could be interesting and relevant as well, when explaining changes in photosynthetic efficiency, for example the chlorophyll or carotenoid content in a leaf.

1.6.1. Chlorophyll fluorescence

Chlorophyll fluorescence can give many information about the physiological status of a plant, for example under stress conditions such as drought, cold or different light irradiances [29]. But what is it exactly? Fluorescence is a type of radiation chlorophylls emit when releasing energy at the excited state. Two different processes can quench the energy otherwise emitted as fluorescence: photochemical quenching (qP), related to the proportion of open PSII reaction centers, and non-photochemical quenching (NPQ) [29]. NPQ is a

process given by different components which the plant can activate within seconds to prevent photodamage; its fastest component (qE) is a mechanism participating to the dissipation of excess energy as heat, acting on light harvesting complexes and involving xanthophylls cycle and transmembrane ΔpH in the thylakoids [15]. Taking qP and qE into account, a decrease in fluorescence emission can be related to an increased photochemical quenching (an increase in open PSII reaction centers and in the electron transport rate from PSII to PSI) or to an increase in qE, when more energy is dissipated as heat [15].

In leaves, thermal dissipation activates with light; dark-adapted leaves have the lowest degree of thermal dissipation and, additionally, all the quinones (Q_A) serving as the primary stable electron acceptor for PSII are oxidized either because of the darkness or because at the very low irradiances normally used to excite chlorophyll fluorescence there is no measurable net reduction of Q_A . Under these conditions the fluorescence yield (F_o) reflects a state of maximum light-use efficiency for PSII photochemistry [30].

When applying a flash of saturating light (for values around $8000 \mu\text{mol photons/m}^2\text{s}$, 0.8 - 1 s) on a dark adapted leaf, photochemical processes do not start because the light pulse is too short and the same happens for heat dissipation. All the energy is then dissipated as fluorescence (maximum fluorescence yield, F_m). F'_o is instead the minimum fluorescence observed after a saturating pulse. In presence of actinic light -a light intense enough to induce photosynthesis (up to $2000 \mu\text{mol photons/m}^2\text{s}$)- the total fluorescence yield obtained when using a saturating pulse (F'_m) will always be lower than F_m (dark-adapted state). This because part of the energy will not be dissipated anymore via fluorescence, but used for photochemistry or dissipated via the qE mechanism instead [31].

As already said, qP relates to the proportion of open PSII reaction centers, in fact it is PSII, rather than PSI, to be responsible for the variable rise in fluorescence emission. qP is given by the formula:

$$qP = \frac{F'_m - F_s}{F'_m - F'_o}$$

The PSII quantum yield (ϕ_{PSII}) differs from qP as it is a measure of the light proportion used by PSII for photochemistry. It is established on light adapted leaves according to the formula:

$$\phi_{PSII} = \frac{F'_m - F_s}{F'_m}$$

Knowing qP in relation to ϕ_{PSII} can be informative as, for example, a decrease in qP can indicate that more reaction centers were closed by saturating light and it could explain a decrease in PSII quantum yield [REF]. Even though, this relation is not straightforward since other mechanisms (e.g. qE) act in the process. As already mentioned, PSII is more prone to photodamage than PSI; when photodamage occurs, the quantum yield of PSII can be reduced and F_v/F_m (PSII maximum quantum yield) is considered a good indicator to assess the state of PSII. A decrease in F_v/F_m indicates possible damage to PSII and a possible change in the efficiency of qE [29]. The PSII maximum quantum yield is calculated as follows:

$$F_v/F_m = \frac{F'_m - F_o}{F'_m}$$

1.6.2. rETR in relation to ϕ_{PSII} and ϕ_{CO_2}

PSII quantum yield was shown to have a linear relation with PSII noncyclic rETR (relative Electron Transport Rate), the electron transport happening between PSII and PSI reaction centers. In our case, we will mainly refer to rETR, calculated as follows:

$$rETR = \phi_{PSII} * PPFD$$

The CO₂ quantum yield (ϕCO_2) can also be considered directly proportional to rETR [30]. Nonetheless, While the linear relation between rETR and ϕPSII seems to be usually consistent, it is not the case with CO₂ assimilation. The reason is that, after light is absorbed by chlorophylls and converted into proton motive force, the energy then available as ATP can actually be used in processes competing with the fixation of CO₂ or less efficient than the Calvin-Benson Cycle at fixing it. Photorespiration is one of the processes actually disrupting a possibly linear relation between ϕCO_2 and rETR (or ϕPSII) [30]. Estimating ϕCO_2 from rETR is always possible, but under certain conditions the estimation is based on strong assumptions about the underlying photochemical processes, such as an equal efficiency of PSII and PSI [15,30]. For example, mild drought leading to stomatal closure and to higher O₂ concentrations in the chloroplasts can cause photorespiration without altering the linear electron transport rate between PSII and PSI [32]. Therefore, when the direct measure of ϕCO_2 is not an option, it is preferable to refer to rETR (or ϕPSII) instead, although this will be a measure relative to the efficiency of PSII only and not to the fixation of CO₂. This holds especially for measurements taken in the field, where non-optimal conditions of environmental variables such as temperature or water availability may trigger photorespiration.

1.6.3. Modeling rETR

The rETR curve is generally characterized by a rapid increase of rETR for low light intensities, until light saturation where rETR_{max} is reached. Asymptotic models (e.g. Michaelis-Menten curve), where rETR is maximum for infinite light intensities, are often used for describing the dependency of rETR from PPFD, when photoinhibition is not present [31]. Waiting-in-line models are also suitable and can also describe the eventual decrease in rETR [33]. According to the waiting-in-line model described and used by Ritchie et al. [33], the rETR curve can be described as follows:

$$\text{rETR} = \frac{(\text{rETR}_{\text{max}} * \text{PPFD})}{\text{PPFD}_{\text{opt}}} * e^{\frac{1-\text{PPFD}}{\text{PPFD}_{\text{opt}}}}$$

Where PPFD_{opt} is the optimum light irradiance at which rETR_{max} is reached and rETR_{max} is a scaling constant for the maximum height of the curve. Nonlinear functions often require starting values for the parameters that will be estimated, in this case PPFD_{opt} and rETR_{max} that can be retrieved by simply plotting the raw data for rETR against PPFD [33].

In controlled environments it is much easier to use techniques, such as fluorescence imaging, that describe PSII efficiency for the whole plant at once and for several plants in very brief time-window [12]. Instead, field studies are more likely to use measurements on single leaves, yet allowing the estimation of the rETR curve from the data. One example is the study of Rascher et al. [34], where field measurements for ϕPSII were taken with a PAM fluorometer on light and dark adapted leaves (for 30s and 30min). The study showed that the three curves obtained under these different conditions usually differed in the maximum rETR that is reached by the plant, but not in the shape of the curve.

As already mentioned, when studying ϕPSII or rETR it is important to gather a high number of observations [10], repeating the measurements at different moments during the day, and at different moments during the plant cycle; when measuring the whole plant is not possible, it can be useful to measure multiple leaves for each plant too. Having repeated measurements enhances the power of the analysis to execute on the data and, in this case, gives a better idea of PSII efficiency in the whole plant. On the other hand, it also favors pseudo replication and correlation problems in the error terms. Pseudo replication can occur for example if more leaves of one plant are measured, when the plant is the measurement unit; this can be overcome by averaging over leaves for the dependent variable, when there is no apparent effect due to the position of the leaf on the stem. Instead, correlation in the error term is possible when repeatedly measuring the same unit on different days. As reported by Peek et al. [35], mixed models can take into account the repetition of measurements by including fixed and random effects, for which the error terms are estimated differently. Moreover, mixed models can support linear and non-linear functions, allowing an easier analysis of response-

curves such as the light response curve. An example of mixed model used for analyzing photosynthesis data is the one specified in the work of Flood et al. [12] where ϕPSII was measured for different genotypes. The “genotype” factor was introduced in the model as fixed effect when comparing the genotypes’ mean responses for ϕPSII while, among the random factors, blocks were taken into account.

1.6.4. Chlorophylls and carotenoids content

Chlorophyll a and b play an important role in light harvesting and energy transfer at the photosystems level. Despite this, the relation between chlorophyll content and photosynthetic efficiency, in particular PSII efficiency, is not always linear as was observed by Campostrini et al (2005), but a general decrease in chlorophyll content was observed with increasing light irradiances [16,27]. Moreover, chlorophyll content has been related to nitrogen content and water use efficiency, with chlorophyll content sometimes linearly related to nitrogen content [7]. This is one more reason for taking this parameter into account, besides PSII efficiency. Therefore, even if the relation between chlorophyll content and photosynthetic efficiency is not straightforward, looking at chlorophylls can help to better understand the state of the plants during the measurements. For the same purpose, the carotenoids content can be relevant, as xanthophylls, synthesized from beta-carotene, are involved in the qE mechanism.

Gas-chromatography is a highly reliable technique for measuring pigments content, but it is also destructive and takes time. Instead SPAD fluorometers allow for taking indirect measurements by using light of different wavelengths in order to measure the reflectance of the leaf and the leaf thickness. The chlorophyll content is calculated on these two values and it is given in SPAD units. These measurements are considered to be quite reliable in different studies [20,36], even if the same studies showed some discrepancies for high SPAD chlorophyll values and values obtained when extracting chlorophyll from the leaf; the relation among the two kinds of measurements was not linear after a certain threshold. Anyhow, for having a feel of the overall chlorophyll content of a leaf, SPAD readers are widely used and considered reliable enough for field surveys; their use is easy and relatively low cost. In our case the SPAD measurement were taken with a MultispeQ [37] together with PSII measurements.

2. Research aim and questions

The aim of this research is to describe different *Cleome gynandra* accessions coming from Asia and Africa for different photosynthetic traits, in particular ϕ_{II} and rETR. For the same accessions, variation was already found in terms of carotenoids, tocopherol and chlorophylls production; moreover, another study on leaf venation is ongoing for the same accessions. Both these traits are also related to photosynthetic processes or used to describe the C4 photosynthetic type.

Other studies already established the capacity of different Arabidopsis genotypes to adapt to different growth irradiances by measuring ϕ_{II} , along with other parameters [10,17,27]. The results were interestingly showing that variation exists for adaptation to different light regimes.

Since variation was found for many traits in Cleome, and being Cleome a C4 species closely related to Arabidopsis, we wanted to investigate its natural variation for photosynthetic efficiency. The plants were measured manually with a MultispeQ and in a climate chamber using the Phenovator system. The aim of these two experiments was to answer the following questions:

1. Is there phenotypic variation for rETR among different Cleome accessions?
2. Do African and Asian accessions respond differently to irradiance variations?
3. Do the two methods used (MultispeQ and Chlorophyll fluorescence imaging) give convergent results?
Is the variation observed (if any) the same for the two methods?

The experiment involving the Phenovator system did not develop as planned since it was the first time Cleome was grown under such conditions; nonetheless, while doing this experiment we had at least the chance to execute some germination trials.

3. Material and Methods

3.1. Data acquisition

The first experiment took place at the Alterra greenhouse (Unifarm-WUR, Netherlands), starting from the first week of February; the second experiment was set in B6, a climate chamber of Radix Climax, starting from the last week of May and lasting one month.

3.2. Plant material

Our collection consists of 73 *Cleome gynandra* accessions. The accessions from West Africa (Benin, Togo and Ghana) have been provided by the Horticulture and Genetics Unit of the Faculty of Agronomic Sciences, University of Abomey-Calavi. The accessions from East Africa and Asia were provided by the World Vegetable Centre (AVRDC). Among the accessions there is also one reference line from South America. All the accessions were planted in the same greenhouse together with a line of *Tarenaya hassleriana*, a C3 species also belonging to the family Cleomaceae. In a study executed at WUR involving the whole set of accessions (Deedi), the accessions showed different pigments contents (carotenoids and chlorophylls). In particular, three clusters were obtained from a PCA analysis with low (1), intermediate (2) and high (3) carotenoids and chlorophylls content, the third cluster only containing African accessions and the first cluster mostly composed by Asian accessions. In the following pictures, the black color will be used for indicating the 1st cluster, the red color for the 2nd cluster and the green color for the 3rd cluster. For a list of the accessions see Table 2.

3.3. Greenhouse experiment

3.3.1. Experimental design

180 *Cleome gynandra* individuals were grown in the greenhouse, representing 51 of the total 73 accessions available; not all the seeds planted were in fact able to germinate. We chose to measure 10 out of 51 accessions planted, representative of the three clusters already mentioned (for details see Table 2). The greenhouse had a North-South orientation and a total of 8 gutters, each one hosting maximum 36 plants (18 per side), so we used a Complete Randomized Block Design (CRBD), with North-South oriented blocks (one block per gutter with 5 blocks in total). Within each block, 1 replicate for each of the 10 measured accessions was randomly positioned (for more details see Figure 1, Appendix).

The sampling was repeated for 6 days, starting from the 3rd week after the plants' germination day. Each day the plants were sampled twice, morning and afternoon. The measurements were then randomized within the blocks and the sampling order of the blocks was randomized too.

For each replicate, 3 consecutive top leaves were measured always in the same order; these leaves were labeled from 1 to 3 and the number of the node for each leaf was annotated. Some lines had very delicate or short-lasting leaves, and we had to choose another leaf after two days.

Germination time, number of nodes (up to 9-10), development of secondary branches, flowering time, stem and branch color were also annotated during the plants' growth for each of the 10 accessions.

3.3.1.1. Plant germination and growth

The seeds were germinated in small pots filled with soil (one per accession) and around one week later individual plants were transferred to rockwool blocks (one per plant). Around three weeks later, the plants were transferred to the final greenhouse compartment in rockwool slabs. Both the rockwool blocks and slabs were provided by grodan®. The light in the greenhouse was given by natural light and 6 light bulbs (200 $\mu\text{mol photons/m}^2\text{s}$); the light was turned off at sunset and turned on again 8 hours later. The watering system was automated, with each plant individually watered 4 times per day at regular intervals. The nutrient solution used for this purpose was the Full Tomato (1,2 mmol NH_4 , 7,2 mmol K, 1 mmol P in 1l/solution). The measurements started one week after the transfer, so that the plants could adapt to the new conditions.

The secondary branches of the plants were partially cut off after the last measurement session, in order to prevent an excessive growth that would hamper the management of the plants while selfing or crossing and when harvesting the seeds.

Pollination was executed by detaching one anther from the flower and spreading the pollen on the flower-stigma by using it as a paint-brush.

3.3.2. MultispeQ

For the measurements in the greenhouse, we used a MultispeQ fluorometer version Beta [37]. This instrument can measure different parameters according to the chosen protocol. We have chosen “The One v3.0” (<http://photosynq.org/protocols/the-one-v3-0-phi2-npqt-using-multi-phase-flash>) and “Chlorophyll content SPAD III” (<https://photosynq.org/protocols/chlorophyll-content-spad-multi-thick-leaf-iii?filter=protocols&q=spad>), to measure PSII photosynthetic efficiency (Φ_{PSII}), linear electron transport (rETR) and chlorophyll content (SPAD). The leaves were not dark adapted; according to “The One” protocol F_o' is taken from a short period in the dark after a light pulse and a short far red pulse. The far red causes PSI to open and drain the PSII plastoquinone pool thus opening all the centers at PSII and oxidizing all of Qa. For each measurement, the MultispeQ also registers date and time, temperature ($^{\circ}\text{C}$), light intensity ($\mu\text{mol photons/m}^2\text{s}$), and relative humidity (%). Additionally, the program allows to answer some questions customized by the user before each measurement. In our case the questions were:

- The block's number where the plant is located
- The number of the plant (coincident with a specific line)
- The leaf that is measured (leaves marked with a label)

The MultispeQ is easily controlled via the relative application that can be installed on a computer or tablet. The data are kept in the memory of the device or directly uploaded to the PhotosynQ website [37]. Our data were saved under the project called “Cleome gynandra – A C4 species” (<https://photosynq.org/projects/cleome-gynandra-a-c4-species>).

3.4. Climate chamber experiments – D2 and B6

A climate chamber is a controlled environment where the dispensation of light, water, temperature and nutrient availability can be regulated; the chance these variables will have an unexpected effect on the plants' phenotypic response is then reduced. All the parameters are controlled with an external computer to minimize the disturbance of the plants. In one chamber there are normally 2 tables where the plants can be positioned in 40x40x40mm rockwool blocks. These are placed in a grid with a top-layer of black PVC that gives a good background color for the fluorescence imaging technique used in one of the chambers and prevents the growth of algae. Each board can host 720 plants for a total of 1440 plants. The watering of the two tables is done by two independent nutrient-solution tanks.

The two chambers we used are called D2 and B6; D2 is equipped with normal cameras by which it is possible to take images of the plants growing in the chamber and B6 hosts the Phenovator [12].

3.4.1. Experimental design

For both experiments, we used a CRBD with different numbers of replicates depending on the accession (for D2 and B6 sowing schemes see Figure 2 and 3, Appendix). Each of the two tables in a climate chamber was divided into 3 blocks, with the whole set of accessions randomly distributed within each block.

3.4.1.1. D2 – Germination

This experiment was done with the purpose of describing Gynandra germination on rockwool blocks, in darkness, at 30 $^{\circ}\text{C}$ (for details on the settings see Table 1, Appendix). The accessions used were 71 out of the total 73, due to seed availability (for further details on the accessions used see Table 2). The number of replicates for each accession was chosen according to seed availability, the origin (Africa/Asia) and the germination date of the same accessions in previous experiments. A picture of the plants which germinated was taken 4 days after sowing.

3.4.1.2. B6 – Phenotyping photosynthesis

Due to heterogeneity in germination and growth times for different accessions, and being the first time using the Phenovator system for *Cleome gynandra*, we encountered some difficulties when proceeding with the experiment. Problems arose with the settings of the chamber conditions as well. For the final settings see Table 1, Appendix; for details on the accessions used see Table 1. The number of replicates for each accession was chosen according to the same criteria used for D2. In B6, on the 16th day after sowing, the temperature was measured at the table level for each of the blocks designed for the experiment to check if the black surface was overheating.

3.4.2. Phenovator: details

The system consists of a camera moving along two axes at a maximum speed of 6 m/s. It can take a picture of 12 plants at the same time, for a total of 120 images (1440 plants). ϕ_{II} is measured via fluorescence imaging using pulse amplitude fluorometry (PAM). The actinic light is the climate chamber light, while the saturating pulse (5000 $\mu\text{mol}/\text{m}^2\text{s}$ for 2 seconds) is given by LEDs positioned on the camera head. The F image is obtained by averaging 24 pictures taken during 10s before the saturating pulse, while 6 images are taken and averaged during the saturating pulse giving the F'_m image. The chlorophyll content is measured via leaf reflectance at 700 and 790 nm, while the projected leaf area (a measure of plant's growth) via NIR imaging. These three kinds of measurements can be alternated during the day [12].

PAM and NIR measurements were repeated according to the following scheme:

Time	1:00	5:00	6:30	7:00	8:30	9:00	10:30	12:00	13:00	15:30	16:30	18:00	18:30	21:00	22:30	23:00
Measure	NIR	NIR	SP	SPEC	NIR	PAM	NIR	PAM	NIR	PAM	NIR	NIR	PAM	SPEC	SP	NIR

3.5. Data analysis

The data were analyzed with R v3.3.2 (R Core Team, 2013). R: A language and environment for statistical computing. R Foundation for Statistical Computing, Vienna, Austria. <http://www.R-project.org/>.

For the greenhouse experiment we chose to use a mixed effect model because the measurements were repeated over days, within a day and within a plant. Moreover, the light intensity was not constant and we had a higher observation density for lower light intensities. Mixed models are in fact used to deal with repeated or nested measurements [12,35].

When plotting raw data for rETR against PPFD, the light response curve did not seem to follow the usual trend where, after a rapid increase, rETR asymptotically goes to saturation; in our dataset, the asymptotical trend was not clear. Therefore, we first established a linear relationship between PPFD and rETR (Eq. 1) considering the effect of Date, MoAf (Morning or Afternoon) and Block (Eq.1a). The second step was to establish a nonlinear relationship between the two variables (Eq. 2), always keeping into account the random factors (Eq. 2a). The models were developed using the R (version 3.3.2) and the packages lmer4 (for the linear model) [38] and nlme (for the nonlinear model) [39]. g stands for the nominal variable "Accession" with 10 j levels. When level i equals level j , $1(g_j = g^i)$ equals 1, otherwise 0.

Linear model (fixed effects):

$$rETR_i = \sum_{j=1}^{10} m \cdot 1(g_j = g^i) PPFD_i + \varepsilon_i \quad [Eq. 1]$$

R – code (fixed + random effects):

$$FunL = lmer(rETR \sim 0 + PPFD: Accession + (1|Date: MoAf: Block)) \quad [Eq. 1a]$$

Nonlinear model (according to Ritchie [33], fixed effects):

$$rETR = \sum_{j=1}^{10} \frac{(rETR_{maxj} * PPF D)}{PPFD_{optj}} 1(g_j = g^i) * \exp\left(\frac{1 - PPF D}{\sum_{j=1}^N PPF D_{optj} 1(g_j = g^i)}\right) * v_i \quad [Eq. 2]$$

R- code (using Eq.2 as rfunH, fixed+random effects):

```
Fun2 = nlme(rETR ~ rfunH(PPFD, emax, rmax), fixed = list(emax + rmax ~ Accession),
           random = emax + rmax ~ 1|Date/MoAf/Block) [Eq. 2a]
```

In both cases the random part of the model represented the three nested factors “Date:MoAf:Block”. For the linear model, the significance of the random effects was tested by using the function exactLRT() in the {RLRsim} package [40]. For both models, to test the significance of the variable “Accession”, a model was fitted with PPF D only as fixed effect and then compared using the function anova() in the lme4 and nlme packages to the two models where “Accession” was present as factors in the fixed effect part.

For assessing differences in slope (response to increasing light intensity) between African and Asian accessions, we used the {boot} package [41,42] and the bootstrap function provided at <http://www.ats.ucla.edu/stat/r/dae/melogit.htm>. This way it was possible to calculate estimates for the slopes and obtain bootstrapped 95% CI (1000 simulations, alpha=0.05) from the fitted models. This was done only for the linear model, while we looked at the nonlinear model only qualitatively.

A PCA was executed using the function prcomp() in the {stats} package in R to compare it to the reference PCA (Deedi). The variable used were germination time, flowering time, SPAD, branch color and stem color.

For the climate chambers D2 and B6 the data were analyzed using an ANOVA (aov()) function in the {base} R package), since the light intensity received by the plants was the same throughout the whole experiment.

The graphs were made with the R-package {ggplot2} [43] and {merTools} [44] for the caterpillar plots.

Table 1 - List of all the accessions, their origin and number of replicates used for each experiment. The accessions used in the greenhouse experiment are indicated with an asterisk and a number (*ⁿ). n (from 1 to 3) corresponds to 3 clusters found in a previous analysis based on compounds content (Deedi).

ACCESSION	ORIGIN	REP-GH	REP-D2	REP-B6	ACCESSION	ORIGIN	REP-GH	REP-D2	REP-B6
EAD-15-001	-	0	12	12	TOT6421	Sub-Saharan Africa	4	12	0
F1 7200x8917	Hybrid	3	24	12	TOT6422 ^{*3}	Sub-Saharan Africa	6	36	24
GYN ^{*1}	South America	5	36	48	TOT6435	Sub-Saharan Africa	2	24	36
ODS-15-013	Sub-Saharan Africa	2	12	0	TOT6439 ^{*3}	Sub-Saharan Africa	5	36	0
ODS-15-015	Sub-Saharan Africa	0	12	12	TOT6440	Sub-Saharan Africa	3	24	36
ODS-15-017	Sub-Saharan Africa	0	12	36	TOT6441D	Sub-Saharan Africa	1	0	0
ODS-15-019	Sub-Saharan Africa	1	24	24	TOT6441F	Sub-Saharan Africa	3	24	48
ODS-15-020	Sub-Saharan Africa	0	12	36	TOT6442	Sub-Saharan Africa	3	12	0
ODS-15-037	Sub-Saharan Africa	2	24	12	TOT7196	Southeast Asia	6	12	0
ODS-15-038	Sub-Saharan Africa	2	12	0	TOT7197	Southeast Asia	6	24	24
ODS-15-041	Sub-Saharan Africa	0	12	0	TOT7198	Southeast Asia	5	24	48
ODS-15-044	Sub-Saharan Africa	0	24	0	TOT7199 ^{*1}	Southeast Asia	8	24	24
ODS-15-049	Sub-Saharan Africa	0	12	0	TOT7200SC	Southeast Asia	3	24	48
ODS-15-054	Sub-Saharan Africa	2	12	0	TOT7441 ^{*1}	Southeast Asia	7	36	12
ODS-15-056	Sub-Saharan Africa	0	12	0	TOT7449	Southeast Asia	1	24	12
ODS-15-059	Sub-Saharan Africa	0	12	12	TOT7462	Southeast Asia	3	24	24
ODS-15-061	Sub-Saharan Africa	0	12	48	TOT7486	Southeast Asia	7	24	36
ODS-15-065	Sub-Saharan Africa	3	24	24	TOT7505	Southeast Asia	1	12	0
ODS-15-075	Sub-Saharan Africa	0	12	36	TOT8887	Sub-Saharan Africa	2	24	12
ODS-15-100	Sub-Saharan Africa	0	12	0	TOT8888	Sub-Saharan Africa	3	24	12
ODS-15-104	Sub-Saharan Africa	0	12	12	TOT8889 ^{*3}	Sub-Saharan Africa	6	36	48
ODS-15-117	Sub-Saharan Africa	0	12	0	TOT8890	Sub-Saharan Africa	3	24	36
RW-SF-10	Sub-Saharan Africa	3	24	24	TOT8891	Sub-Saharan Africa	3	12	12
TOT1048	Southeast Asia	3	36	48	TOT8892	Sub-Saharan Africa	3	24	24
TOT1100 (Tar)	-	3	36	48	TOT8915	Sub-Saharan Africa	5	36	48
TOT1480	Southeast Asia	0	12	0	TOT8916	Sub-Saharan Africa	3	0	0
TOT3514	Southeast Asia	0	12	12	TOT8917	Sub-Saharan Africa	5	12	0
TOT3527	Southeast Asia	5	24	12	TOT8918 ^{*3}	Sub-Saharan Africa	5	24	24
TOT3534SC	Southeast Asia	1	24	24	TOT8925G ^{*2}	Sub-Saharan Africa	4	36	24
TOT3536	Southeast Asia	6	12	36	TOT8925P	Sub-Saharan Africa	3	24	36
TOT4447	South Asia	0	12	0	TOT8926	Sub-Saharan Africa	0	12	12
TOT4489	South Asia	0	12	0	TOT8931	Sub-Saharan Africa	4	24	36
TOT4935	Southeast Asia	0	12	48	TOT8933	Sub-Saharan Africa	3	24	36
TOT4937 ^{*2}	Southeast Asia	7	36	24	TOT8996	East Asia	3	24	36
TOT4976	Southeast Asia	0	12	12	TOT8997	East Asia	1	24	36
TOT5799SC	Southeast Asia	0	12	24	TOT8998	East Asia	3	12	0
TOT6420	Sub-Saharan Africa	3	24	0	-	-	-	-	-

4. Results

4.1. Greenhouse experiment

4.1.1. rETR

4.1.1.1. A note on the dataset

In general, *Cleome gynandra* is a tropical species and therefore used to quite high temperatures and light intensities [7,8]. Despite this, the greenhouse experiment conducted here at WUR took place during winter, with an average light intensity and temperature of about $300\mu\text{mol}/\text{m}^2\text{s}$ and 18°C . These possibly suboptimal conditions may be the cause of the unusual relation observed between increasing PPFD and rETR. Whereas the relation is generally curvilinear, with rETR going to saturation after a certain light intensity, the pattern observed in this experiment for rETR only showed a slight curvature without apparently going to saturation (Figure 1A). Another cause for the unusual relation between rETR and PPFD could be due to imprecision of the measuring tool (MultispeQ [37]), for which too high or too low light intensities may result in distorted values for ϕPSII and consequently rETR. In Figure 1B it is possible to look at the two overlaid histograms for rETR and PPFD, binned according to the variable "Date:MoAf:Block". Higher mean values for PPFD correspond to higher mean values for rETR and it does not seem that there are problems concerning the tool. Despite this, without doing further experiments on the MultispeQ performance at extreme values for PPFD, it is difficult to say if this is due to the instrument used for the measurements or to long-term adaptation mechanisms in the plants. Assuming that the measurements taken for rETR dependent on PPFD are not biased by technical issues, a straight line was shown to fit well the variation characterizing our dataset (Eq.1), but also a nonlinear model was fitted (Eq.2).

4.1.1.2. Linear model

The mixed effect model described by Equation 1, was characterized by a random intercept for the nested variable "Date:MoAf:Block". The nested variable explained 95% of the total variance for the random part of the model; including this variable was assessed as significant (10000 simulations, $\text{LRT}=626.01$, $p < 2.2\text{e-}16$) by using a likelihood ratio test based on simulation [40].

Including the factor "Accession" in the fixed part of the model resulted in a lower BIC ($\text{BIC} = 4066.3$) than for the model where PPFD only was included for the fixed part (Equation 1, $\text{BIC} = 4170.8$), meaning that the inclusion of the factor was significant ($p = 4.16\text{e-}08$). The slopes' mean values for the interaction

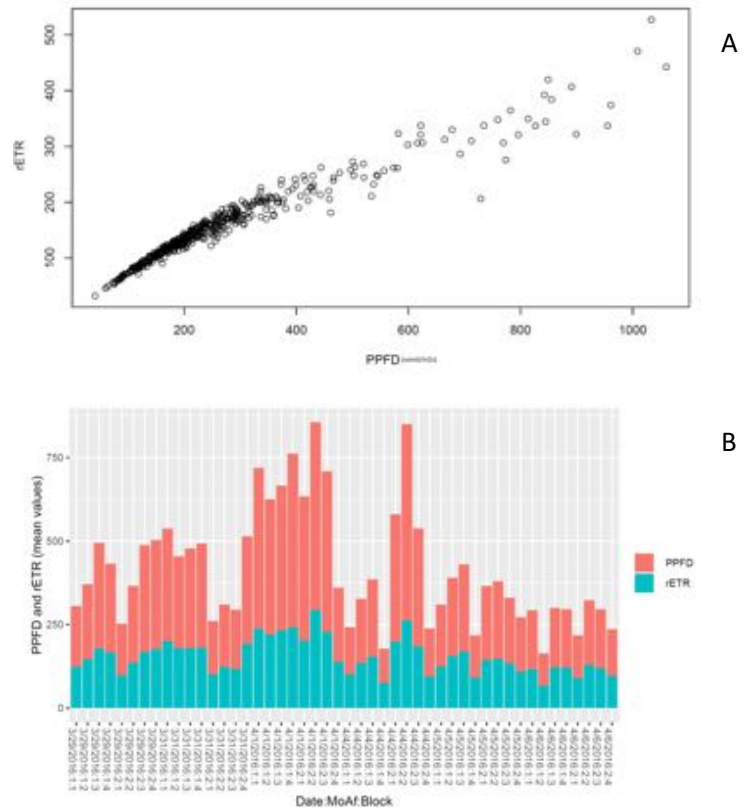


Figure 1 - In Figure A, the raw data for rETR are plotted against PPFD. It is possible to notice a slight curvature. In Figure B, the mean values for PPFD and rETR binned according to the variable "Date:MoAf:Block" are shown in an overlaid histogram.

“PPFD:Accession” and their bootstrapped confidence intervals (1000 simulations, $\alpha=0.05$) are reported in Table 2 (see also Figure 2A and B). The accessions 4937 (Asian) and 8889 (African) had the highest and lowest coefficients for the slope (respectively $\beta = 0.419$, SE = 0.008, n=48 and $\beta = 0.338$, SE = 0.008, n=48). Accessions were established to be different when the bootstrapped

Table 2 - Estimates and bootstrapped 95% CI for slope coefficients from Eq. 1a. For all the accessions n=48.

Accession	Cluster (Deedi)	Origin	Estimates		Bootstrap		
			β (slope)	SE	β (slope)	2.5%	97.5%
8889	3	Africa	0.338	0.008	0.342	0.292	0.39
6439	3	Africa	0.367	0.007	0.372	0.334	0.422
8915	1	Africa	0.371	0.007	0.374	0.333	0.416
8925G	2	Africa	0.389	0.007	0.39	0.357	0.421
6422	3	Africa	0.389	0.01	0.391	0.352	0.435
8918	3	Africa	0.391	0.008	0.395	0.358	0.43
7199	1	Asia	0.399	0.008	0.403	0.371	0.445
7441	1	Asia	0.414	0.008	0.416	0.39	0.45
4937	2	Asia	0.419	0.008	0.418	0.383	0.452
GYN	1	South America	0.385	0.007	0.391	0.354	0.445

confidence intervals for each slope (Table 2) were not overlapping. In general, the three Asian accessions (4937, 7199, 7441) had the higher coefficient for rETR, while three of the African accessions (6439, 8915, 8889) had the lower coefficient (Figure 2A and B).

4.1.1.3. Nonlinear model

The nonlinear model described by Equation 2 was again characterized by random intercepts for the nested variable “Date:MoAf:Block” for the two parameters $rETR_{max}$ and $PPFD_{opt}$. The factor “Accession” was significant ($p < 0.0001$) when comparing the model including the factor (BIC = 3698.141) to the model without the factor (BIC = 3903.886). As obtaining bootstrapped coefficients for $rETR_{max}$ and $PPFD_{opt}$ was not possible for time constraints, we present only the estimates for each accession and the respective plot (Table 3, Figure 2C). In general, it seems that the results obtained with the nonlinear model agrees with the results from the linear model. The accessions with a higher $rETR_{max}$ were the Asian ones (4937, 7199, 7441), while the ones with the lowest $rETR_{max}$ were some of the African accessions (8889, 6439, 8915).

Table 3 - Estimates for $rETR_{max}$ and $PPFD_{opt}$ found modeling $rETR$ according to Ritchie. Line 4937 was taken as intercept, therefore, to calculate the estimates for each accession, the value for 4397 has to be added to any of the other values.

Parameter	$rETR_{max}$					$PPFD_{opt}$					
	Accession	Value	Std.Error	DF	t-value	p-value	Value	Std.Error	DF	t-value	p-value
4937 (Int)		1912.2199	130.3528	411	14.669574	0	524.0058	29.63909	411	17.67955	0
6422		-898.1879	133.39117	411	-6.733488	0	-221.892	28.78692	411	-7.70809	0
6439		-713.516	124.04145	411	-5.752238	0	-178.996	26.65664	411	-6.71488	0
7199		51.4725	147.43406	411	0.349122	0.7272	11.1859	31.75746	411	0.35223	0.7248
7441		-138.6351	144.82904	411	-0.957233	0.339	-33.6843	31.12388	411	-1.08226	0.2798
8889		-724.5444	128.76398	411	-5.626918	0	-197.982	27.45885	411	-7.21013	0
8915		-470.1295	132.2215	411	-3.555621	0.0004	-129.514	28.08847	411	-4.61092	0
8918		-455.7801	135.01026	411	-3.375892	0.0008	-115.524	28.96411	411	-3.9885	0.0001
8925G		-165.2772	153.95643	411	-1.073532	0.2837	-76.886	31.74455	411	-2.42202	0.0159
GYN		-448.4544	128.34175	411	-3.494221	0.0005	-108.008	27.54641	411	-3.92096	0.0001

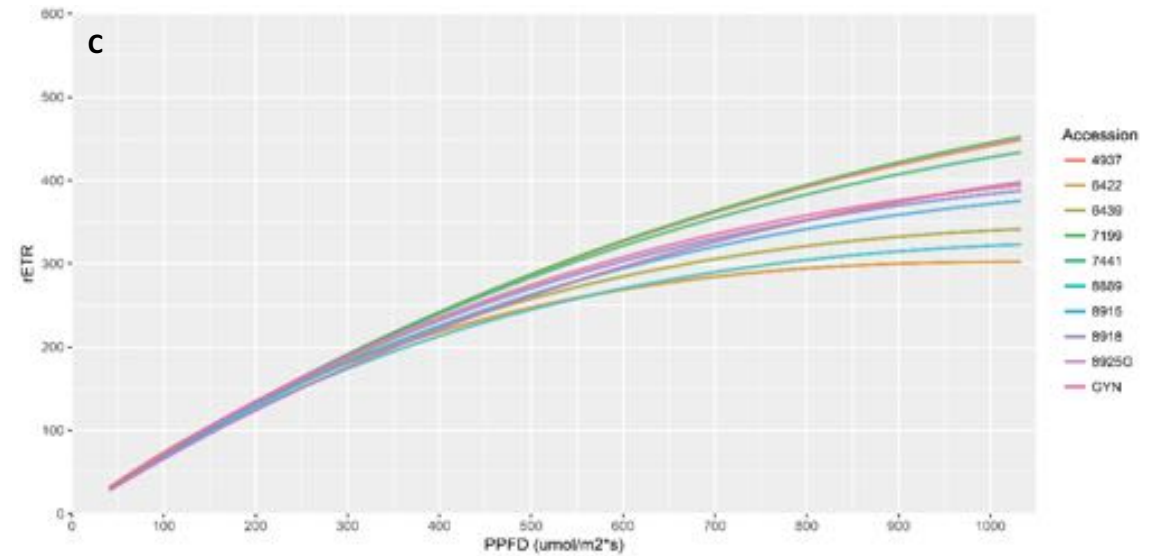
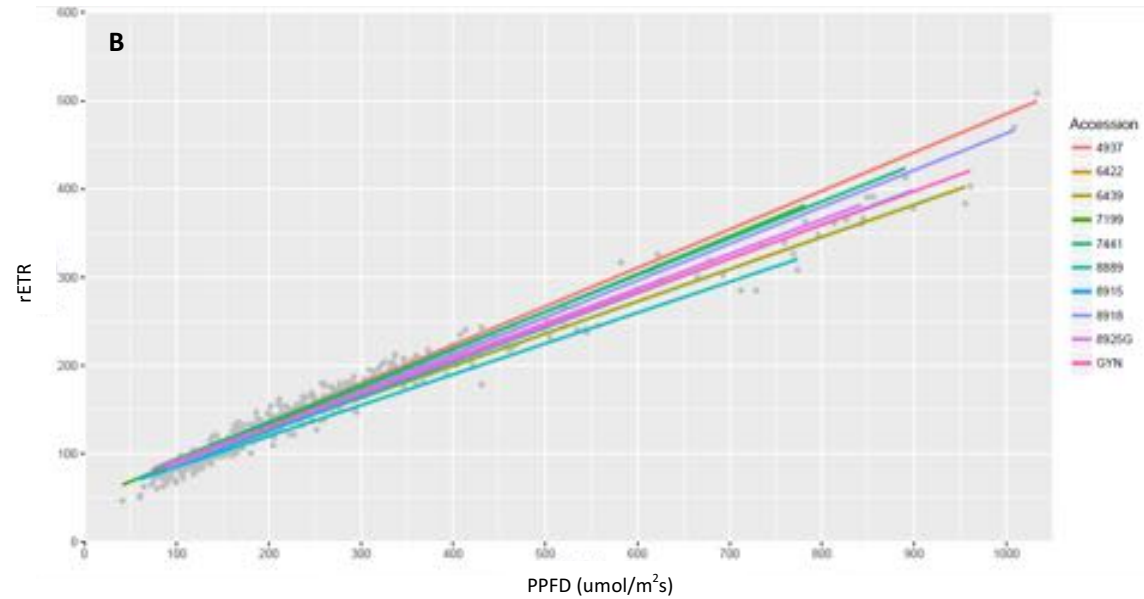
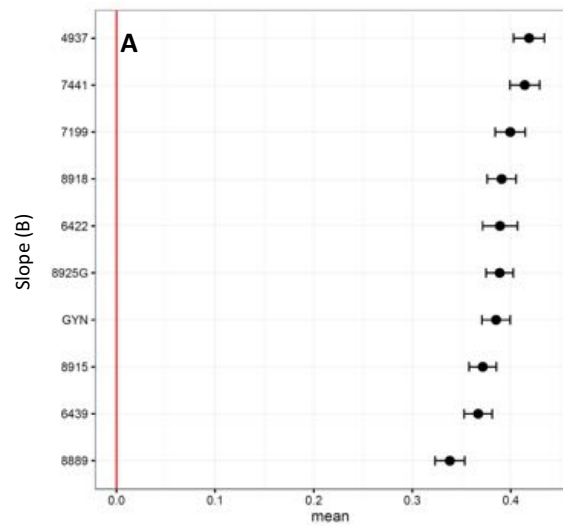


Figure 2 – A. Representation of slope coefficient estimates with estimated 95% intervals from Eq. obtained with bootstrapping. Non overlapping CI were used for testing differences between accessions. B. Fitted lines for each accession from Equation 1a. The slopes were described by the fixed part of the model, where a common intercept was specified. C. Fitted lines for each accession from Equation 2a. $rETR_{max}$ and $PPFD_{opt}$ were described by the fixed part of the model, where a common intercept was specified.

4.1.2. PCA

For the principal components analysis, the following variables were taken into account:

- Germination and flowering time
- Chl content (SPAD)
- Stem and branch color

The first component of the PCA was explaining 46% of the variance, while the second and third components were explaining 25% and 13% of the total variance, for a total of 84% (see Table 2, Appendix).

To see if the same clusters were found as in the reference PCA (Deedi), we used these 3 first axes and see how the 10 accessions measured in the greenhouse were placed in the 3D-space so obtained (see Figure 3). For example, when considering first and second components, the Asian accessions and GYN showed late flowering and reduced Chl content if compared to the African accessions.

As in the reference PCA, looking at the first component, flowering time was inversely proportional to Chl content, germination and all the other variables considered.

A correlation matrix was in fact calculated for these variables to establish their level of correlation (Table 4). Chl content (SPAD), was highly and positively correlated with stem color ($r = 0.66$), while flowering time had a weak correlation with all the other variables (r ranging from -0.29 to 0.23).

Traits	SPAD	Germination	Flowering	Stem	Branch
SPAD	1.00	0.45	-0.16	0.66	0.44
Germination		1.00	0.23	0.36	0.22
Flowering			1.00	-0.19	-0.29
Stem Color				1.00	0.34
Branch Color					1.00

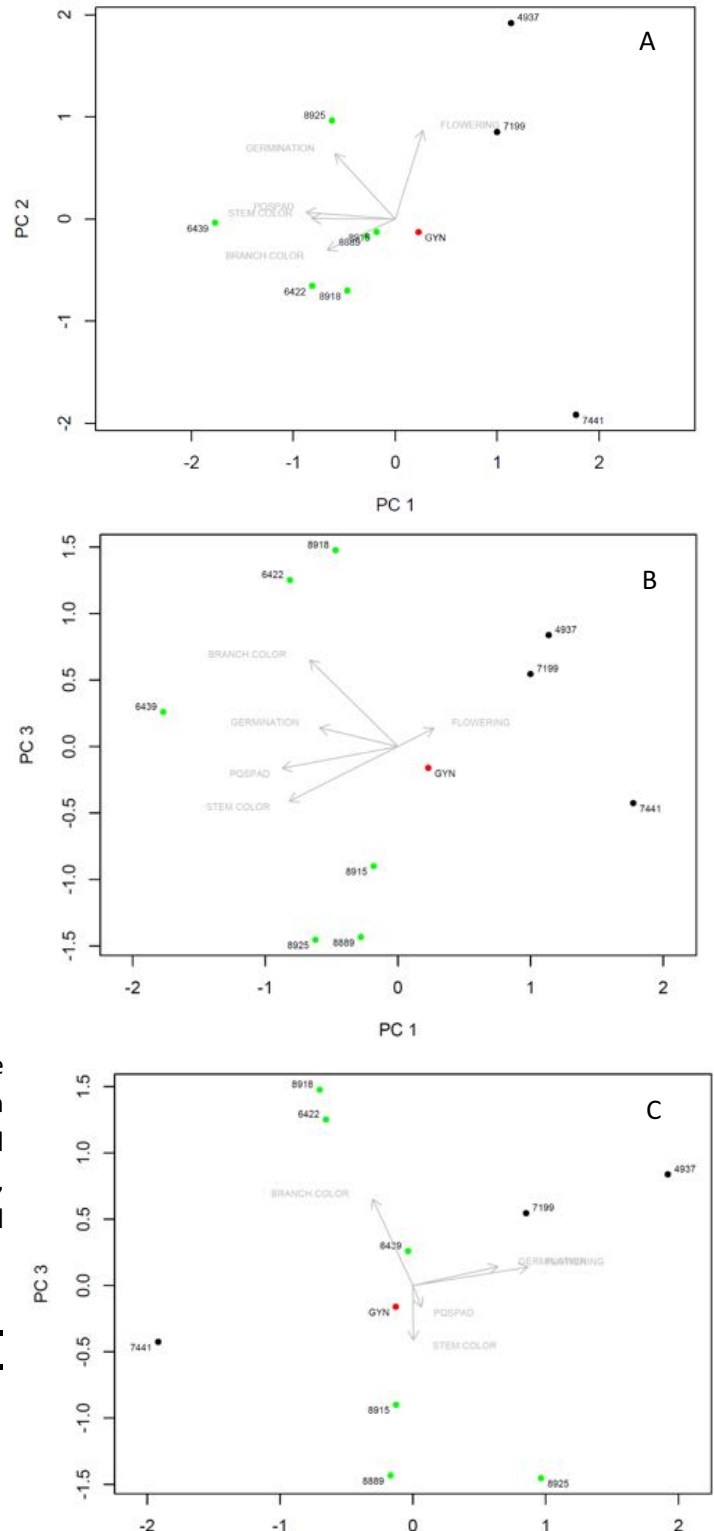


Figure 3 – A, B, C biplots for the first three components of the principal component analysis (PC1 explains ~50% of the total variance). The color assigned to the different accessions are based on the accession provenience (red = South America, green = Africa, black = Asia).

4.1.3. SPAD - Chlorophyll content

The chlorophyll content for the 10 accessions analyzed in the greenhouse was measured as SPAD using the MultispeQ. The one-way ANOVA test executed for SPAD yielded significant variation among different accessions ($F(9, 459) = 35.43, p < 2e-16$). The SPAD mean value for each accession is reported in Table 3, Appendix. A Tukey post-hoc test ($\alpha = 0.05, HSD = 3.28$) showed which accessions were actually differing for SPAD. The accessions were grouped as indicated in Figure 4. For some accessions, such as 6439 and 8889, the standard deviation was larger ($sd = 6.7$ and $sd = 6.4$), indicating a higher dispersion of the data.

4.2. D2 and B6 experiment

4.2.1. Germination

For the experiment in B6, the ANOVA test done for assessing differences in germination showed that the only significant factor in determining differences in germination was “Accession”, while introducing factors such as “Block” or “Table” did not improve the model fit; a One-Way ANOVA was used to assess differences in germination for the 3rd day after sowing ($F(50, 205) = 8.092, p < 2e-16$) and the 4th day after sowing ($F(50, 205) = 9.289, p < 2e-16$). The same happened for the experiment in D2, where only “Accession” was used as factor in a One-Way ANOVA ($F(70,285) = 4.634, p < 2e-16$).

71 accessions were used for D2, whilst for B6 only 51 accessions were used due to seed availability. The germination percentage in D2 was of 42% after 3 days in the dark at 30°C, 3 days after sowing. the germination percentage in B6 was of 27% 3 days after sowing and 30% 4 days after sowing. In B6, the treatment at 30°C in the dark was given for one day only, 1 day after sowing (see Table 1, Appendix).

In D2, the lines with a germination rate higher than 50% were 28. Among these, there were both African and Asian lines, but also the hybrid F1 7200x8917 and GYN (see Figure 4, Appendix). Some lines that performed relatively well in D2 (e.g. 7441, 4937) with a germination rate of 50% or higher, had a much lower germination % in B6 (10% or lower). The line of *Tarenaya hassleriana* included in the experiment (accession 1100), showed a low germination rate in both trials (0% D2 and 6% B6).

It is to notice that some problems occurred during the germination phase in the climate chamber experiments. In D2, a higher percentage of plants germinated, but the seedlings had very weak stems and were not able to survive after germination for 4 days in the dark. In B6, there were problems with the chamber settings, and optimal germination conditions were provided for a shorter time than planned. Moreover, the reasons for an overall low germination % in both trials can be different. First, the seeds were germinated directly on Rockwool and, despite a preliminary trial, there was no previous experience

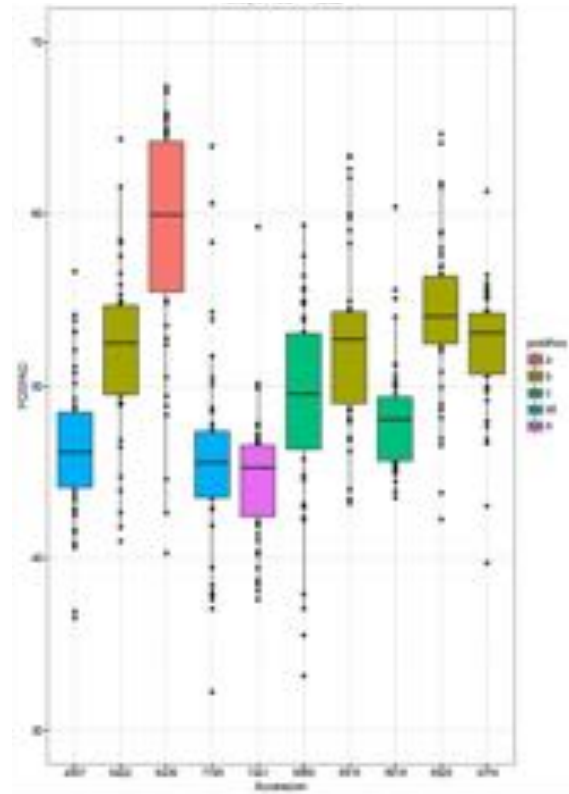


Figure 4 - Boxplot for SPAD. Each box is colored depending on the post-hoc group to which the accession belongs (Table 3, Appendix).

with Cleome germination on rockwool. Second, from the literature we knew that 30°C for 4 days in the dark were enhancing germination and that exposure to light was hampering the germination of Cleome seeds [45], but we were not sure of the effect under our experimental setup. Third, the seeds were harvested at different times, thus had different ages; some were even the original seeds from the collection made available by the initial providing institutions (University of Abomey-Calavi and AVRDC).

4.2.2. Temperature in B6

On the 16th day after sowing, the temperature in B6 was measured at the table level (see Figure 5). The temperature set for the chamber was 23°C, but at the table level the mean temperature measured was 35.78°C (SE = 0.21°C).

The raise of temperature to 27°C at the end of the experiment in B6 seemed to stress the plants, even if the watering regime was intensified (see Table 1, Appendix). In fact, it was possible to observe a principle of yellowing for many of the accessions (Figure 6). This could be related to the fact that the black PVC layer overheats and to the way Cleome handles high temperatures.

T1		T2	
30.7	32.5	32.2	28.1
30.7	31.9	32.5	27.8
33	30.5	31.9	31.8
Door			

Figure 5 - Mean temperature (°C) at the table surface for the 6 blocks designed for the experiment in B6. The temperature was taken at two different points for each block. The blocks' colors are the same as in Figure 1 and 2, Appendix.

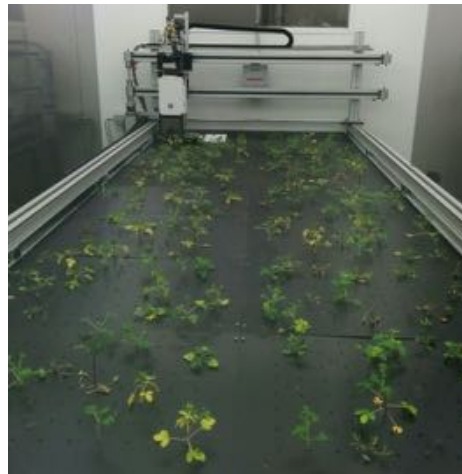


Figure 6 - Cleome plants in the climate chamber B6 during the 30C treatment. Some of the plants show a principle of yellowing.

5. Discussion

The first part of the discussion mainly deals with findings coming from the greenhouse experiment conducted for this study, where rETR and SPAD were measured for ten *Cleome* accessions. The second part treats of various issues occurred during the experiment relative to fluorescence imaging in the climate chamber, and indications on how to overcome these problems in a practical way.

5.1. Differences between African and Asian lines

This study shows that phenotypic variation is present for different traits in *Cleome gynandra*. In particular, *Cleome* accessions seem to cluster, or differentiate, according to their geographical origin (Africa or Asia) for several traits. The phenotypic variation found here and in previous studies (Deedi) for photosynthetic traits makes *Cleome* even more interesting when thinking of it as a possible C4 model [2,4]. Population structure and adaptation to different environments may be the cause for the differences between the two groups. This has to be considered when moving from phenotyping to genomic studies. In fact, when for example conducting a GWAS on the African and Asian populations of *Cleome* for a particular trait, the genetic background of these two populations may be a confounding factor together with the environment [46].

Here, *Cleome* was studied for rETR, chlorophyll reflectance (SPAD) and other traits. In a linear relation between light intensity and rETR (Equation 1 and 1a), it seems that Asian lines (7441, 7199, 4937) respond with a higher rETR coefficient to a given light intensity than some of the African lines (8915, 6439, 8889) (Table 2 and Figure 2A,B). In a nonlinear relation between PPFD and rETR (Equation 2 and 2a), rETR for the same Asian accessions seems to get to saturation for much higher light intensities than for the African lines mentioned above (Table 3, Figure 2C), but this could not be formally tested. The PCA analysis executed for other traits (SPAD, germination, flowering, stem and branch color), also indicates that accessions from the same country group together according to the first component explaining about 50% of the variation present (Figure 3A, B; Table 2, Appendix). A difference between Asian and African lines for photosynthetic traits is in line with a previous study (Deedi). Differences between the two geographical groups were found for the production of compounds related to photosynthetic processes (chlorophylls, xanthophylls, tocopherols) and other traits (Deedi); Asian accessions were in fact found poorer than African accessions in chlorophylls and carotenoids, but richer in tocopherols. Here, we found that Asian lines have a lower SPAD than African lines (Figure 4; Table 3, Appendix), where SPAD is a proxy for the relative chlorophyll content of a leaf [20,36].

5.2. rETR

In this study, plants were measured under “field” conditions meaning that, besides providing artificial light at 200 $\mu\text{mol}/\text{m}^2\text{s}$, also natural light was acting in the greenhouse. As a result, steady-state photosynthesis could only be assumed, as it is done when taking field measurements without dark-adapting leaves [11]. This has the advantage of capturing the photosynthetic performance of a plant under real field conditions where light is constantly varying, but there are also pitfalls.

Highly controlled light conditions are most of the times an advantage (e.g. when doing genetic/genomic studies to reduce environmental noise) to the point that works following the approach used for this thesis are not many [34,47]. In fact, several studies [12,26,27] measure chlorophyll fluorescence on leaves where photosynthesis is actually at its steady state (because the leaves were acclimated to a stable light

intensity) or on leaves where all the reaction centers are at first open (if the leaves were dark-adapted). This means that, considering short term adaptation only, all plants have to a certain extent stabilized their energy use for photochemical and nonphotochemical processes at the moment of the measurement [29].

Natural light intensity was quite variable during the two weeks where the greenhouse measurements were taken for this experiment (Figure 1B). Hence, different measurements may have been taken at moments where some of the plants were dissipating more energy than at the steady-state via mechanisms such as NPQ. As a result, one could argue that this study is not comparable with studies where plants were first acclimated to a given light intensity before measuring [12,27]. On the other hand, Rascher et al. [34] measured PSII quantum yield and rETR on leaves under ambient light conditions in the field and then measured the same leaves after dark-adapting them. They noticed that the rapid light curves for the different species measured were either overlapping or offset for a constant value; in particular, leaves not adapted to dark had higher values for rETR or ϕ_{II} relative to dark-adapted ones for the same PPFD [34]. Our measurements could as well be characterized by an offset value, given the conditions under which they were taken, but they are still valid for relative comparisons and for having an idea of the variation found for rETR within the species.

5.2.1. Cleome and Arabidopsis

Assuming that the measurements for this study were taken when photosynthesis was at the steady state, we will compare Cleome with Arabidopsis for rETR. rETR, together with ϕ_{II} , has been used to observe the PSII response in different genotypes or to different treatments (e.g. light variation, water stress, nitrogen deficiency) in C3 species, especially Arabidopsis [12,27], or in C4 species, for example Corn [26].

Phenotypic variation for rETR in response to increasing irradiance was found in Arabidopsis [27]. In this case, Arabidopsis was acclimated to increasing light intensities and then measurements were taken. As already said, the results regarding Arabidopsis [27] cannot be compared in strict terms to the results of the present study. Nonetheless, here we observed that for higher light intensities, there seemed to be a larger phenotypic variation for rETR in Cleome (ranging from about 1000 to 2000 $\mu\text{mol}/\text{m}^2\text{s}$). The variation observed among different Arabidopsis genotypes for rETR was also found to be larger for higher light intensities, for example in plants grown at 100 $\mu\text{mol}/\text{m}^2\text{s}$ and then acclimated to increasing light intensities [27]. On the other hand, in this case rETR_{max} had a narrower range than the value found in Cleome (Figure 2C, Table 3), approximately from 550 to 650 $\mu\text{mol}/\text{m}^2\text{s}$ [27].

5.2.2. Why such a high rETR_{max}?

The extremely large phenotypic variation found within the species *Cleome gynandra* and the high rETR_{max} found for different Cleome lines can be due to two main aspects of a.) measurement techniques and methodology and b.) growing conditions.

First, the instrument MultispeQ may have not been correctly calibrated, or its light sensor may work less precisely for higher light intensities, but also taking measurements manually could have played a role. This indeed has to be checked and might partially explain the high rETR_{max} values found for Cleome in general. As already said, Rascher et al. [34] also noticed that for some species measured under field conditions rETR is positively offset relative to rETR for dark adapted leaves; this may partially contribute to such high values for rETR in our case, but it should not influence the way the rapid light curve for each Cleome accession is positioned relative to the others. The greatest variation in rETR was found between Asian and African lines of Cleome that a previous study (Deedi) already assessed as different for the production

of photosynthetic compounds. Hence, such a large variation for rETR may be due to imprecision in the instrument or in the measurements themselves, but part of this variation also seems to be related to the plants' phenotypes.

Second, C₄ species are generally more efficient than C₃ under high temperatures or light intensities [8,13,22], but in our experiment Cleome was probably grown under nonoptimal conditions, meaning under a lower light intensity and, to a lesser extent, temperature (Table 4, Appendix), compared to its natural habitat (Table 5 and 6, Appendix). Studies done on C₄ species grown under low light mainly



Figure 7 – Cleome plants grown in the greenhouse for the experiment presented in this report. The plants were spaced at a constant distance in the greenhouse, but it is still possible to notice the dense canopy characterizing Cleome.

focus on leaf anatomy, carbon isotopes partitioning, assimilation and CO₂ leakiness [48,49], while less often parameter such as ETR are considered [50]. Yet, these studies show that C₄ species can adapt to low light conditions by different mechanisms depending on the species observed. A hypothesis on why some C₄ species need to be able to adapt to low irradiances is that these species often develop dense canopies [51]. Cleome canopy for example is quite dense, especially for Asian accessions (see Figure 7). This may explain to a certain extent the high values measured for rETR under suboptimal conditions; Cleome phenotype could be plastic and adaptable to low light intensities. It may explain why Asian accessions, with a denser canopy, showed a higher rETR_{max} relatively to African accessions under the possibly low light irradiance at which they were grown.

5.3. Pigments and photosynthesis

Chlorophylls and carotenoids are essential pigments in plant photosynthesis. They are involved in light-harvesting and energy transfer, constituting antenna complexes together with other proteins. Additionally, Chl_a is also present at the reaction centers of PSII and PSI and carotenoids, in particular Xanthophylls, are involved in photoprotection [14,15,19,20]. A previous study on three population of Arabidopsis [16] found that QTLs for ϕ_{II} were collocated with QTLs for chlorophyll reflectance for two of the three populations analyzed in the study, indicating a possible common genetic origin for the two traits. Furthermore, chlorophyll content or reflectance per leaf area positively correlated with photosynthetic capacity, as also shown in other studies [52]. On the contrary, we found that plants with a lower chlorophyll reflectance (Asian) have a higher rETR coefficient (Figure 2 & 4).

Looking at the origin of the accessions and historical time series for climatic data, it seems that Asian accessions originate from areas characterized by a.) a lower annual PPFD than accessions from Africa and b.) a wider range of light intensities throughout the year (5 and 6, Appendix). Moreover, our plants were probably grown under much lower light intensities (200 $\mu\text{mol}/\text{m}^2\text{s}$ on average) than what could be an average PPFD in the subtropics. A hypothesis could be that African accessions have evolved coping with higher light intensities than Asian accessions. Hence, they may respond with a much higher production of chlorophylls and carotenoids when grown in suboptimal light conditions, still without being able to fully express their potential in terms of rETR. It would be interesting to collect data about production of photosynthetic pigments for the same accessions growing in their origin places or under natural

conditions. Another explanation could be that there are differences between mechanisms of short term adaptation to high light intensity between Asian and African accessions. In fact, if Asian plants produce more tocopherols, African accessions produce more violaxanthin (Deedi). While tocopherols are mainly involved in the scavenging of ROS, reactive oxygen species formed under (light) stress [53], violaxanthin de-epoxidation (xanthophyll cycle) is a process involved in quenching of excess energy [15].

5.4. Climate chamber experiments

Obtaining fluorescence imaging data from on PSII efficiency and leafy reflectance measured in the controlled conditions of a climate chamber would have been highly valuable to explain/validate observations within the greenhouse and thus enabled more precise comparisons with other studies. The data were gathered, but not analyzed, since many problems were encountered during the experiment. The dataset produced was in the end based on a relatively low number of plants and yet, requiring a laborious manipulation because of overlapping leaves entering the picture frame of other plants.

Despite the unsuccessful data collection, it was the first time Cleome was grown in B6 (and D2), making this experience useful for future experiments. Being the first time, there was no previous experience about Cleome germination on Rockwool blocks or about the rapidity by which the seedlings would have developed in this substrate. Literature was only available for Cleome germination only about light and temperature requirements for Cleome seeds [23]. Another unknown factor was the number of plants that could be fit in the chamber without leaves overlapping after a few days of growth, since the system was built for Arabidopsis [12], much flatter and smaller than Cleome.

A CRB design as the one we have used here is still advisable, but for a first run less lines shall be grown in B6, with more replicates. Our maximum number of replicates per line per block was 8, but 15 is more likely to be a good number of replicates. In this respect, it is also advisable to select lines that show a germination percentage of at least 50% (see Figure 4, Appendix). Regarding the height of the camera, this can be adjusted while the plants are growing, but the height at which this is fixed above the table must be signed down. Another aspect to consider is that the black covers applied above the Rockwool block seem to overheat, especially for high light conditions (Figure 5 and 6), so the temperature at the table level will be higher than in the room on average.

According to what said above, here are some indications for growing Cleome on rockwool blocks in a climate chamber:

Step	Notes	Light	Temperature	Water
Sowing	<ul style="list-style-type: none"> Rockwool blocks must be used upside down. A shallow hole can be made at the bottom of each block with the woody tip of a paintbrush. Seeds must be stuck with a paintbrush to the side of the hole 			<ul style="list-style-type: none"> The rockwool blocks must be soaked in half ro full tomato solution before sowing
Germination	<ul style="list-style-type: none"> The following conditions are to be applied for 24 consecutive hours. While more than 24 hours of darkness seem to promote an excessive elongation of the young stem, a temperature of 30°C may be applied for a longer time. 	<ul style="list-style-type: none"> Dark 	<ul style="list-style-type: none"> 30 °C 	<ul style="list-style-type: none"> No watering needed
Growth	<ul style="list-style-type: none"> Temperature or light intensity may be varied during the course of the experiment. 	<ul style="list-style-type: none"> 8am – 20pm: 400 umol/m2s 20pm – 8am: dark 	<ul style="list-style-type: none"> Less than 23°C 23°C were used for this experiment, but the temperature at the table level was on average 35°C 	<ul style="list-style-type: none"> Watering every 2 days with Full Tomato solution

5.5. Further developments

From this work it is clear that African and Asian accessions differ in the way they process light at the level of PSII. Different directions could be taken from here. First, it is necessary to measure the same plants under more stable light conditions (e.g. in a climate chamber such as B6) or by repeating the experiment in the greenhouse while keeping some plants in a climate chamber as a control. For example, this would allow to test if the rETR values observed here are offset as observed in previous work for chlorophyll measurements taken under field conditions and compared to measurements taken on dark-adapted leaves [34]. Second, with respect to a previous experiment (Deedi), it would be interesting to look in detail at how rETR and photosynthetic pigments relate when thinking of physiological and adaptational mechanisms characterizing African and Asian lines. Third, another interesting aspect would be to link rETR to CO₂ assimilation and biomass production as this could be used for improving Cleome when thinking of it as a leafy vegetable [1,25].

In general, measuring the same lines at steady-state photosynthesis would also allow to make stricter comparisons with the closely related *Arabidopsis* for chlorophyll measurements, to better understand how C3 and C4 photosynthesis differentiate. Moreover, the same parameters considered in this study could be observed in other C3 and C4 species closely related to *Cleome gynandra*. The genus *Cleome* and the Cleomaceae family have been studied already in evolutionary, anatomical and physiological terms [4,6,54]. Linking all this information is also an essential step to take if *Cleome* wants to be used as a C4 model [2].

6. Conclusions

Here, we have shown that *Cleome gynandra*, a C4 species, is phenotypically variable for photosynthetic traits such as rETR and chlorophyll reflectance. This variability is in particular linked to the geographical origin of *Cleome*, with Asian and African lines differing for these traits. This geographical pattern is interesting when considering different aspects: the adaptational and evolutionary history of *Cleome*, the potential of this variation in *Cleome* breeding and the relevance it can have in the study of C3 and C4 photosynthesis.

REFERENCES

1. Chweya J a, Mnzava N a. Cat's whiskers. International Plant Genetic Resources Institute. 1997.
2. Brown NJ, Parsley K, Hibberd JM. The future of C4 research - Maize, Flaveria or Cleome? *Trends Plant Sci.* 2005;10: 215–221. doi:10.1016/j.tplants.2005.03.003
3. Schranz ME, Mitchell-Olds T. Independent ancient polyploidy events in the sister families Brassicaceae and Cleomaceae. *Plant Cell.* 2006;18: 1152–1165. doi:10.1105/tpc.106.041111
4. Marshall DM, Muhaidat R, Brown NJ, Liu Z, Stanley S, Griffiths H, et al. Cleome, a genus closely related to Arabidopsis, contains species spanning a developmental progression from C3 to C4 photosynthesis. *Plant J.* 2007;51: 886–896. doi:10.1111/j.1365-313X.2007.03188.x
5. Barker MS, Vogel H, Schranz ME. Paleopolyploidy in the Brassicales: analyses of the Cleome transcriptome elucidate the history of genome duplications in Arabidopsis and other Brassicales. *Genome Biol Evol.* 2009;1: 391–9. doi:10.1093/gbe/evp040
6. van den Bergh E, Kulahoglu C, Brautigam A, Hibberd JM, Weber APM, Zhu XG, et al. Gene and genome duplications and the origin of C4 photosynthesis: Birth of a trait in the Cleomaceae. *Curr Plant Biol. Elsevier B.V.;* 2014;1: 2–9. doi:10.1016/j.cpb.2014.08.001
7. Ghannoum O, Evans RJ, von Cammerer S. Nitrogen and Water Use Efficiency of C4 Plants. In: Govindjee, Sharkey, editors. *Advances in Photosynthesis and Respiration.* Springer; 2003. pp. 129–146. doi:10.1007/978-1-62703-447-0
8. Sage RF. The evolution of C 4 photosynthesis. *New Phytol.* 2004;161: 341–370. doi:10.1046/j.1469-8137.2004.00974.x
9. Murchie EH, Pinto M, Horton P. Agriculture and the new challenges for photosynthesis research. *New Phytol.* 2009;181: 532–552. doi:10.1111/j.1469-8137.2008.02705.x
10. Harbinson J, Prinzenberg AE, Kruijer W, Aarts MGM. High throughput screening with chlorophyll fluorescence imaging and its use in crop improvement. *Curr Opin Biotechnol. Elsevier Ltd;* 2012;23: 221–226. doi:10.1016/j.copbio.2011.10.006
11. Kuhlger S, Austic G, Zegarac R, Osei-Bonsu I, Hoh D, Chilvers MI, et al. MultispeQ Beta: a tool for large-scale plant phenotyping connected to the open PhotosynQ network. *R Soc Open Sci.* 2016;3. doi:10.1098/rsos.160592
12. Flood PJ, Kruijer W, Schnabel SK, Schoor R Van Der, Jalink H, Snel JFH, et al. Phenomics for photosynthesis , growth and reflectance in Arabidopsis thaliana reveals circadian and long - term fluctuations in heritability. *Plant Methods. BioMed Central;* 2016; 1–14. doi:10.1186/s13007-016-0113-y
13. Zhu XG, Long SP, Ort DR. What is the maximum efficiency with which photosynthesis can convert solar energy into biomass? *Curr Opin Biotechnol.* 2008;19: 153–159. doi:10.1016/j.copbio.2008.02.004
14. Hallik L, Niinemets Ü, Kull O. Photosynthetic acclimation to light in woody and herbaceous species: A comparison of leaf structure, pigment content and chlorophyll fluorescence characteristics measured in the field. *Plant Biol.* 2012;14: 88–99. doi:10.1111/j.1438-8677.2011.00472.x
15. Ruban A V., Johnson MP, Duffy CDP. The photoprotective molecular switch in the photosystem II antenna. *Biochim Biophys Acta - Bioenerg. Elsevier B.V.;* 2012;1817: 167–181. doi:10.1016/j.bbabi.2011.04.007
16. Flood JP. Natural genetic variation in Arabidopsis thaliana photosynthesis - Chapter 1, 2 & 4. Wageningen University. 2015.
17. Flood PJ, Harbinson J, Aarts MGM. Natural genetic variation in plant photosynthesis. *Trends Plant Sci. Elsevier Ltd;* 2011;16: 327–335. doi:10.1016/j.tplants.2011.02.005
18. Murchie EH, Niyogi KK. Manipulation of photoprotection to improve plant photosynthesis. *Plant*

- Physiol. 2011;155: 86–92. doi:10.1104/pp.110.168831
19. Hogewoning SW, Wientjes E, Douwstra P, Trouwborst G, van Ieperen W, Croce R, et al. Photosynthetic Quantum Yield Dynamics: From Photosystems to Leaves. *Plant Cell*. 2012;24: 1921–1935. doi:10.1105/tpc.112.097972
 20. Netto AT, Campostrini E, De Oliveira JG, Bressan-Smith RE. Photosynthetic pigments, nitrogen, chlorophyll a fluorescence and SPAD-502 readings in coffee leaves. *Sci Hortic (Amsterdam)*. 2005;104: 199–209. doi:10.1016/j.scienta.2004.08.013
 21. Gowik U, Westhoff P. The path from C3 to C4 photosynthesis. *Plant Physiol*. 2011;155: 56–63. doi:10.1104/pp.110.165308
 22. Edwards EJ, Smith S a, Thresholds CE. The Origins of C 4 Grasslands: Integrating Evolutionary and Ecosystem Science. *Science (80-)*. 2010;328: 587–590. doi:10.1126/science.1177216
 23. Wasonga DO. Phenotypic Characterization of Kenyan and South African Spider Plant (*Cleome gynandra* L.) Ecotypes. University of Nairobi. 2014.
 24. Royal Botanic Gardens Kew. SEPASAL database. In: 1999 [Internet]. [cited 2 Jan 2016]. Available: <http://apps.kew.org/sepasalweb/sepaweb>
 25. Schonfeldt HC, Pretorius B. The nutrient content of five traditional South African dark green leafy vegetables-A preliminary study. *J Food Compos Anal*. 2011;24: 1141–1146. doi:10.1016/j.jfca.2011.04.004
 26. D’Ambrosio N, Arena C, Virzo De Santo A. Different relationship between electron transport and CO2 assimilation in two Zea mays cultivars as influenced by increasing irradiance. *Photosynthetica*. 2003;41: 489–495. doi:10.1023/B:PHOT.0000027512.82632.7c
 27. van Rooijen R, Aarts MGM, Harbinson J. Natural genetic variation for acclimation of photosynthetic light use efficiency to growth irradiance in *Arabidopsis*. *Plant Physiol*. 2015;167: 1412–29. doi:10.1104/pp.114.252239
 28. Zhu XG, Ort DR, Whitmarsh J, Long SP. The slow reversibility of photosystem II thermal energy dissipation on transfer from high to low light may cause large losses in carbon gain by crop canopies: A theoretical analysis. *J Exp Bot*. 2004;55: 1167–1175. doi:10.1093/jxb/erh141
 29. Maxwell K, Johnson GN. Chlorophyll fluorescence--a practical guide. *J Exp Bot*. 2000;51: 659–668. doi:10.1093/jexbot/51.345.659
 30. Baker NR. Chlorophyll fluorescence: a probe of photosynthesis in vivo. *Annu Rev Plant Biol*. 2008;59: 89–113. doi:10.1146/annurev.arplant.59.032607.092759
 31. Ralph PJ, Gademann R. Rapid light curves: A powerful tool to assess photosynthetic activity. *Aquat Bot*. 2005;82: 222–237. doi:10.1016/j.aquabot.2005.02.006
 32. Cornic G, Fresneau C. Photosynthetic carbon reduction and carbon oxidation cycles are the main electron sinks for photosystem II activity during a mild drought. *Ann Bot*. 2002;89: 887–894. doi:10.1093/aob/mcf064
 33. Ritchie RJ. Photosynthesis in the Blue Water Lily (*Nymphaea Caerulea* Saligny) Using Pulse Amplitude Modulation Fluorometry. *Int J Plant Sci*. 2012;173: 124–136. doi:Doi 10.1086/663168
 34. Rascher U, Liebig M, Lüttge U. Evaluation of instant light-response curves of chlorophyll fluorescence parameters obtained with a portable chlorophyll fluorometer on site in the field. 2000; 1397–1405.
 35. Russek-cohen MSPE, Wait DA, Forseth IN. Physiological response curve analysis using nonlinear mixed models. 2002; 175–180. doi:10.1007/s00442-002-0954-0
 36. Uddling J, Gelang-Alfredsson J, Piikki K, Pleijel H. Evaluating the relationship between leaf chlorophyll concentration and SPAD-502 chlorophyll meter readings. *Photosynth Res*. 2007;91: 37–46. doi:10.1007/s11120-006-9077-5
 37. David Kramer’s Lab MSU. PhotosynQ [Internet]. Available: <https://photosynq.org/>
 38. Douglas Bates, Martin Maechler, Ben Bolker SW. Fitting Linear Mixed-Effects Models Using lme4.

- J Stat Softw. 2015;67(1): 1–48.
39. Pinheiro J, Bates D, DebRoy S, Sarkar D, Heisterkamp S, Van Willigen B. Package “nlme” - Linear and Nonlinear Mixed Effects Models. 2017.
 40. Scheipl, F., Greven, S. and Kuechenhoff H. No Title. *Comput Stat Data Anal.* 2008;52(7): 3283–3299.
 41. Ripley AC and B. boot: Bootstrap R (S-Plus) Functions. R package version 1.3-18.
 42. Davison, A. C. & Hinkley D V. *Bootstrap Methods and Their Applications.* Cambridge Univ Press. 1997;
 43. Wickham H. *ggplot2: Elegant Graphics for Data Analysis.* Springer-Verlag, New York; 2009.
 44. Jared E. Knowles and Carl Frederick. merTools: Tools for Analyzing Mixed Effect Regression Models. R package version 0.2.1. [Internet]. 2016. Available: <https://cran.r-project.org/package=merTools>
 45. Ochuodho JO, Modi AT. Light-induced transient dormancy in *Cleome gynandra* L. seeds. *African J Agric Res.* 2007;2: 587–591. Available: <http://www.academicjournals.org/AJAR>
 46. Vilhjálmsson BJ, Nordborg M. The nature of confounding in genome-wide association studies. 2013; doi:10.1038/nrg3382
 47. Osei-bonsu I, Hoh D, Cruz J, Savage L, Kuhlger S, Teravest D, et al. Variation in chlorophyll fluorescence-derived photosynthetic parameters and SPAD of cowpea genotypes subjected to drought and flooding stress at the pod filling stage. 2016; doi:10.13140/RG.2.1.1663.4007
 48. Bellasio C, Griffiths H. Acclimation to low light by C4 maize: Implications for bundle sheath leakiness. *Plant, Cell Environ.* 2014;37: 1046–1058. doi:10.1111/pce.12194
 49. Ubierna N, Sun W, Kramer DM, Cousins AB. The efficiency of C4 photosynthesis under low light conditions in *Zea mays*, *Miscanthus x giganteus* and *Flaveria bidentis*. *Plant, Cell Environ.* 2013;36: 365–381. doi:10.1111/j.1365-3040.2012.02579.x
 50. Li Q, Deng M, Xiong Y, Coombes A, Zhao W. Morphological and photosynthetic response to high and low irradiance of *aeschynanthus longicaulis*. *Sci World J.* Hindawi Publishing Corporation; 2014;2014. doi:10.1155/2014/347461
 51. Sage RF, McKown AD. Is C4 photosynthesis less phenotypically plastic than C3 photosynthesis? *J Exp Bot.* 2006;57: 303–317. doi:10.1093/jxb/erj040
 52. Takai T, Kondo M, Yano M, Yamamoto T. A quantitative trait locus for chlorophyll content and its association with leaf photosynthesis in rice. *Rice.* 2010;3: 172–180. doi:10.1007/s12284-010-9047-6
 53. Munné-Bosch S. The role of α -tocopherol in plant stress tolerance. *J Plant Physiol.* 2005;162: 743–748. doi:10.1016/j.jplph.2005.04.022
 54. Voznesenskaya E V., Koteyeva NK, Chuong SDX, Ivanova AN, Barroca J, Craven LA, et al. Physiological, anatomical and biochemical characterisation of photosynthetic types in genus *Cleome* (Cleomaceae). *Funct Plant Biol.* 2007;34: 247–267. doi:10.1071/FP06287

APPENDIX

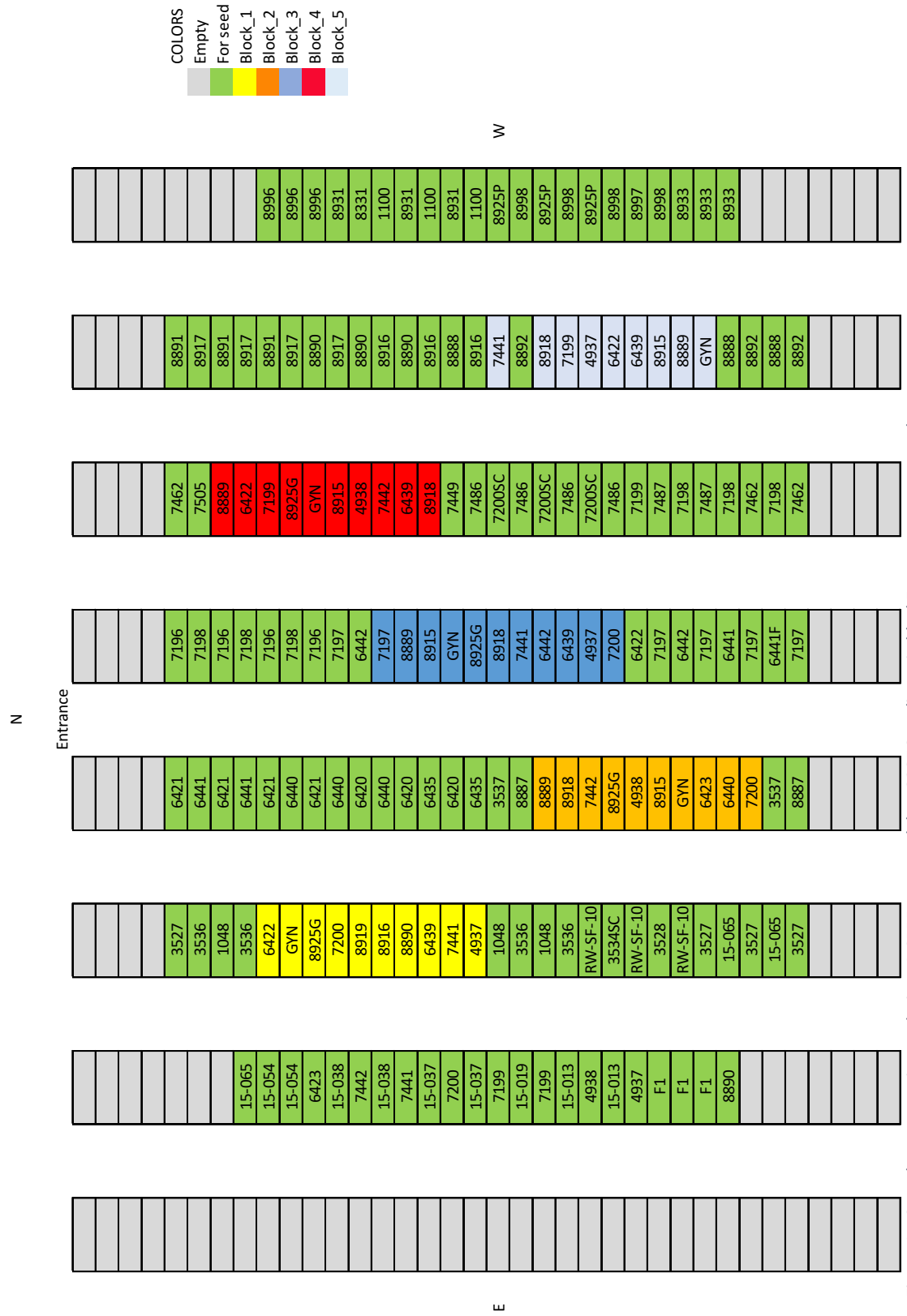


Figure 1 - Greenhouse experiment design. A CRBD was used, but 8925G replicate in block5 was not present at the moment of the measurement. The block was excluded from the statistical analysis.

Table 1 - Growth conditions for experiment in D2 and B6.

Climate Chamber	D2											
Days after sowing	1	1	X	2	2	X	3	3	4	4	X	
Time	20:00 - 08:00	08:00 - 20:00	-	20:00 - 08:00	08:00 - 20:00	-	20:00 - 08:00	08:00 - 20:00	20:00 - 08:00	08:00 - 20:00		
T°C	30	30	-	30	30	-	30	30	30	END		
PPFD (8am-20pm)	0	0	-	0	0	-	0	0	0			
%Humidity	65	65	-	65	65	-	65	65	65			
Watering	X	X	-	X	X	-	V	V	X			
Climate Chamber	B6 - Planned											
Days after sowing	1	1	1	2	2	X	3	3	19	19	23	23
Time	18:00 - 08:00	08:00 - 18:00	18:00 - 20:00	20:00 - 08:00	08:00 - 20:00	-	20:00 - 08:00	08:00 - 20:00	20:00 - 08:00	08:00 - 20:00	20:00 - 08:00	08:00 - 20:00
T°C	30	30	23	23	23	-	23	23	Increasing PPFD or T°C			END
PPFD (8am-20pm)	0	0	400	0	400	-	0	400	65	65	65	
%Humidity	65	65	65	65	65	-	65	65	65	65	65	
Watering	Every 2 days						Every other day					
Climate Chamber	B6 - Executed											
Days after sowing	1	1	1	2	2	2	3	3	19	19	23	23
Time	20:00 - 08:00	08:00 - 16:00	16:00 - 20:00	20:00 - 08:00	08:00 - 16:00	16:00 - 20:00	20:00 - 08:00	08:00 - 20:00	20:00 - 08:00	08:00 - 20:00	20:00 - 08:00	08:00 - 20:00
T°C	21	21	30	30	30	23	23	23	30	30	30	END
PPFD (8am-20pm)	0	200	0	0	0	400	0	400	0	400	0	
%Humidity	65	65	65	65	65	65	65	65	65	65	65	
Watering	Every 2 days						Every other day					

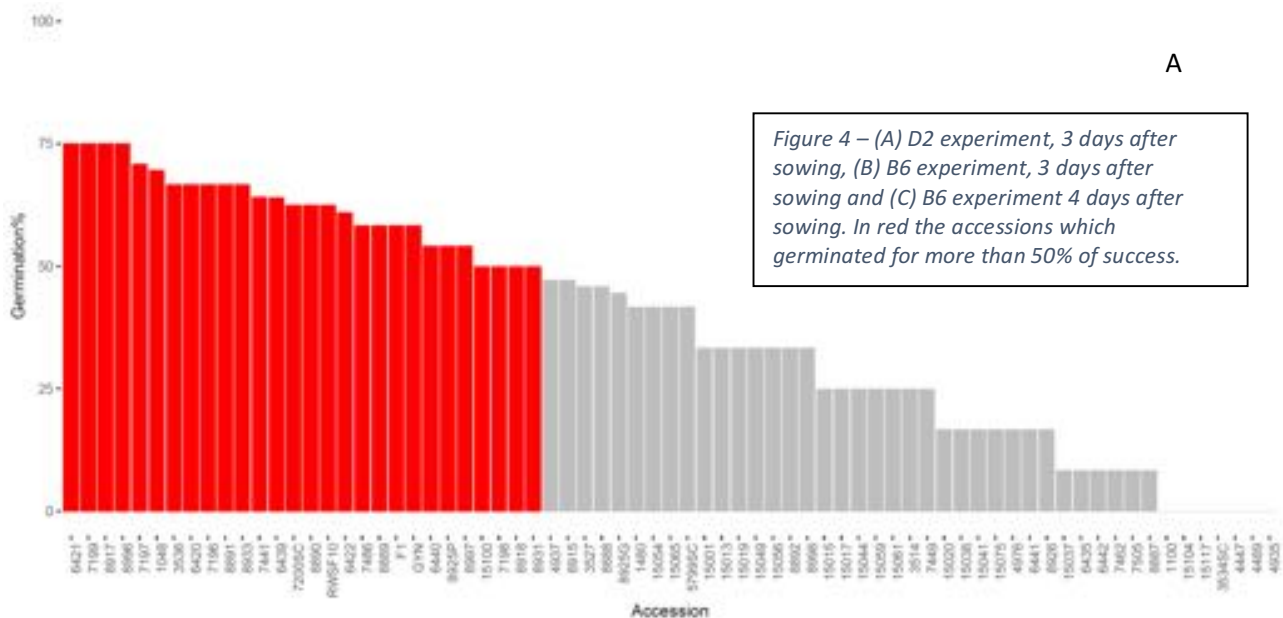
Table 2 - Principal components and the proportion of variance explained by each. The first three components explained 84% of the total variance.

PCA	Comp1	Comp2	Comp3	Comp4	Comp5
Standard deviation	1.517	1.121	0.813	0.675	0.570
Proportion of Variance	0.460	0.251	0.132	0.091	0.064
Cumulative Proportion	0.460	0.712	0.844	0.935	1.000

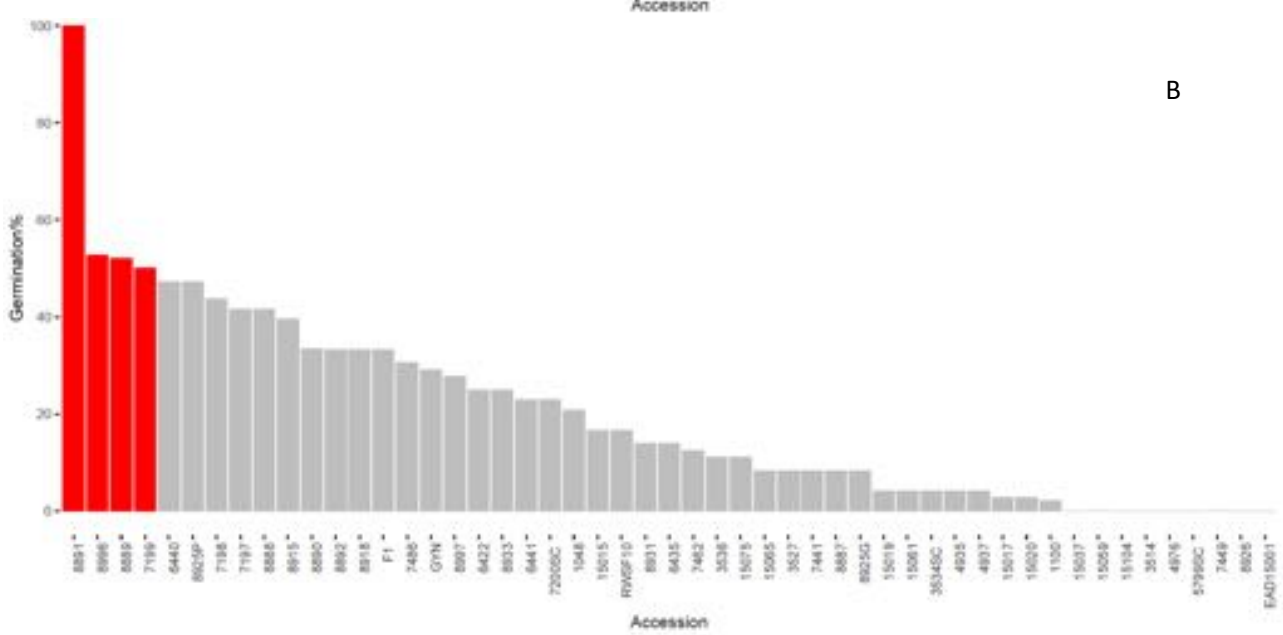
Table 3- SPAD mean values and standard deviations for the 10 accessions used in the greenhouse experiment. The groups determined by a Tukey post-hoc test are reported in the 4th column.

Accession	SPAD	sd	Group
6439	58.8	6.7	a
6422	52.1	4.6	b
8915	52.1	6.1	b
8925	54.2	4.6	b
GYN	52.3	3.6	b
8889	48.5	6.4	c
8918	48.4	3.2	c
4937	46.4	4.2	cd
7199	45.9	5.8	cd
7441	44.8	3.8	d

A



B



C

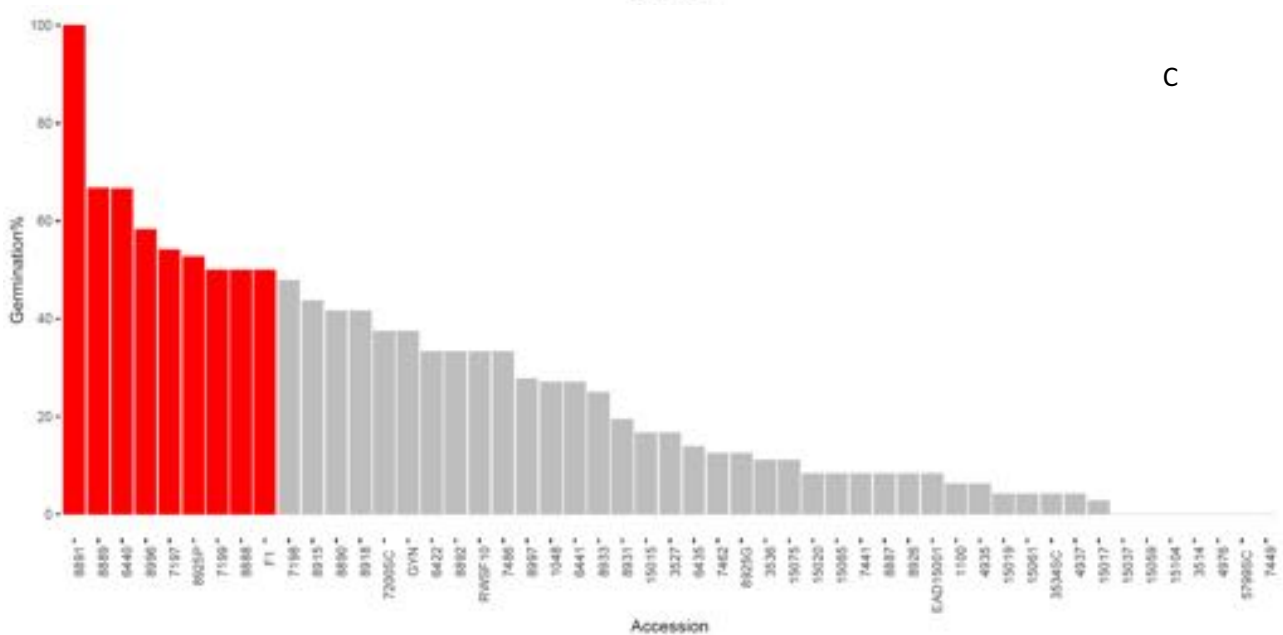


Table 4 – Greenhouse average light intensity ($\mu\text{mol}/\text{m}^2\cdot\text{s}$) and temperature (Celsius). The data were averaged over several measurements taken for each day from the greenhouse internal monitoring system.

Month	Week	PPFD($\mu\text{mol}/\text{m}^2\cdot\text{s}$)	T(*C)
March	1	266.4768	13.81563
	2	197.9653	15.63234
	3	215.7988	15.64479
	4	217.0818	19.76716
April	1	220.1426	20.64068

Table 5 – Climatic data divided per country. The countries are the origin country of the accessions used for this study. The data were retrieved at <http://sdwebx.worldbank.org/climateportal/> (data series from 1961 to 1999, averages are shown) and <http://www.climate-charts.com/world-index.html> (for daylight and humidity).

Country	Temp (*C)	PPFD (photon $\mu\text{mol}/\text{m}^2\cdot\text{s}$)	Daylight	Precipitation (mm)	Humidity (%)
BEN	27.46	975.83	6am-17pm	1034.27	70.25
GHA	27.25	928.96		1184.94	
TGO	26.80	996.12	6am-18pm	1189.11	
KEN	24.50	1075.11	6am-18pm	678.11	56.71
MWI	21.98	1022.86	6am-18pm	1112.29	65.08
RWA	19.01	947.02	6am-18pm	1162.80	
TZA	22.31	1018.01	6am-18pm	1052.38	
UGA	22.60	1109.09		1207.90	
ZAF	17.60	1031.49	4am-20pm//8am-16pm*	474.78	
ZMB	21.58	1096.15	6am-18pm	1004.75	63.24
BGD	25.47	869.90		2266.52	
LAO	23.22	867.29	5am-18pm//6am-17pm	1758.35	74.84
MYS	25.14	932.27	6am-18pm	2992.79	
Taiwan	9.6	764.18	5am-18pm//6am-16pm	38.08	
THA	26.25	957.62	5am-18pm//6am-17pm	1532.48	
AVE	22.72	972.79	Around 12hours light	1245.97	66.02

Table 6 – PPFD divided per country and month. The countries are the origin country of the accessions used for this study. The data were retrieved at <http://sdwebx.worldbank.org/climateportal/> (data series from 1961 to 1999, averages are shown).

C/M	Jan	Feb	Mar	Apr	May	Jun	Jul	Aug	Sep	Oct	Nov	Dec
BEN	1017.48	1083.31	1087.15	1060.94	1006.62	890.30	862.18	837.25	888.38	971.47	999.59	1005.34
GHA	1011.09	1045.60	1043.05	1025.15	963.16	853.87	818.72	772.70	789.95	906.91	959.96	957.40
TGO	1046.24	1124.22	1116.55	1091.62	1027.71	907.55	853.87	817.44	887.10	983.61	1043.69	1053.91
KEN	1144.67	1237.34	1197.08	1074.36	1012.37	959.96	938.23	989.36	1128.69	1099.29	1028.35	1091.62
MWI	979.77	1012.37	1037.30	1003.42	945.90	852.59	873.04	1014.29	1175.35	1225.84	1144.67	1009.81
RWA	931.84	990.00	963.80	938.87	912.03	936.31	995.75	1005.34	990.64	917.78	885.82	896.05
TZA	1106.96	1168.32	1075.64	937.59	853.23	862.18	883.27	954.85	1089.70	1118.46	1081.39	1084.59
UGA	1170.87	1231.59	1184.29	1111.43	1062.22	1008.53	993.20	1057.11	1165.76	1114.63	1079.48	1129.97
ZAF	1356.22	1229.03	1065.42	881.35	739.46	664.69	717.73	862.18	1053.91	1148.50	1303.81	1355.58
ZMB	1005.98	1016.20	1050.72	1089.06	1067.97	1034.74	1083.31	1193.24	1245.01	1227.75	1113.99	1025.79
BGD	810.41	947.82	1071.17	1082.03	1000.23	830.22	778.45	772.70	734.35	818.08	807.21	786.12
LAO	782.29	919.06	1030.26	1077.56	1007.90	853.23	793.79	794.43	850.67	809.77	772.06	716.46
MYS	922.89	1009.81	1029.63	1019.40	954.85	928.01	922.25	916.50	924.17	887.10	846.20	826.38
Taiw	465.28	527.28	636.57	751.61	864.73	1017.48	1201.55	1067.33	881.99	735.63	544.53	476.15
THA	947.18	1053.91	1114.63	1150.42	998.31	912.03	884.54	875.60	881.99	864.09	900.52	908.19

